Modeling boreal forest's mineral soil and peat C dynamics with Yasso07 model coupled with Ricker moisture modifier

Boris Ťupek[1], Aleksi Lehtonen[1], Alla Yurova[2], Rose Abramoff[3,5,9], Stefano Manzoni[4], Bertrand Guenet[5], Elisa Bruni[5], Samuli Launiainen[1], Mikko Peltoniemi[1], Shoji Hashimoto[6], Xianglin Tian[7,8], Juha Heikkinen[1], Kari Minkkinen[7], and Raisa Mäkipää[1]

[1] Natural Resources Institute Finland (LUKE), Helsinki, 00790, Finland

[2] Northwest Institute of Eco-environment and Resources, Lanzhou, 730000, China

[3] Lawrence Berkley National Laboratory, University of California, Berkeley, 94720, USA

[4] Stockholm University, Stockholm, 10691, Sweden

[5] Laboratoire de Géologie, L'École Normale Supérieure (ENS), Paris, 75005, France

[6] Forestry and Forest Products Research Institute (FFPRI), Tsukuba, 305-8687, Japan

[7] Helsinki University, Helsinki, 00014, Finland

[8] College of Forestry, Northwest A & F University, Shaanxi, 712100, China

[9] Ronin Institute, Montclair, New Jersey, 07043-2314, USA

Corresponding author: Boris Ťupek (boris.tupek@luke.fi)

Keywords: soil water content (SWC), heterotrophic respiration, CO_2 emissions, soil organic carbon (SOC), Yasso07 model, environmental modifier, boreal forest

Highlights

20 • The revision of functional water control in soil C and Earth systems models with large data across scales is needed to improve their spatial and temporal projections.

• Substituting the Yasso07 soil C model's original saturation type dependency of decomposition on precipitation with a one parameter hump-shaped Ricker moisture function improved modelled SOC stocks in a catena of mineral and organic/peat soils in boreal forest.

25 • The Ricker moisture function which was set to peak at rate 1 and calibrated against SOC and CO_2 data using Bayesian MCMC approach showed a maximum rate of decomposition in well-drained soils along the forest – mire soil moisture gradient.

• Using forest-mire SOC and CO_2 data together with the moisture data only from the topsoil humus layer in model optimization was crucial to accurately model the spatial SOC increase from mineral soil forests to peatlands.

30 • The functional dependencies based only on soil CO_2 emissions failed to estimate accurate SOC stocks (of forested peatlands) but showed good performance statistics for CO_2 estimates.

Abstract

As soil microbial respiration is the major component of land CO_2 emissions, differences in the functional dependence of respiration on soil moisture among the Earth system models (ESM) contributes significantly to the uncertainties in their

35 projections.

Using soil organic C (SOC) stocks and CO_2 data from a boreal forest – mire ecotone in Finland and Bayesian data assimilation, we revised the precipitation-based environmental function of the Yasso07 soil carbon model. We fit this function to the observed microbial respiration response to moisture and compared its performance against the original Yasso07 model and the version used in the JSBACH land surface model with a reduction constant for decomposition rates in wetlands.

40 The Yasso07 soil C model coupled with the calibrated unimodal moisture function with an optimum in dry soils accurately reconstructed observed SOC stocks and soil CO_2 emissions and clearly outperformed previous model versions on paludified organo-mineral soils in forested peatlands and water-saturated organic soils in mires. The best estimate of the posterior moisture response of decomposition used both measurements of SOC stocks and CO_2 data from the full range of moisture conditions (from dry/xeric to wet/water-saturated soils). We observed unbiased residuals of SOC and CO_2 data modelled with

45 the moisture optimum in well-drained soils, suggesting that this modified function accounts more precisely for the long-term SOC change dependency according to ecosystem properties as well as the contribution of short-term CO_2 responses including extreme events.

The optimum moisture for decomposition in boreal forests was in dry well-drained soils instead of the mid-range between dry and water-saturated conditions as is commonly assumed among soil C and ESM models. Although the unimodal moisture

50   modifier with an optimum in well-drained soils implicitly incorporates robust biogeochemical mechanisms of SOC accumulation and CO_2 emissions, it needs further evaluation with large scale data to determine if its use in land surface models will decrease the uncertainty of projections.

Graphical abstract
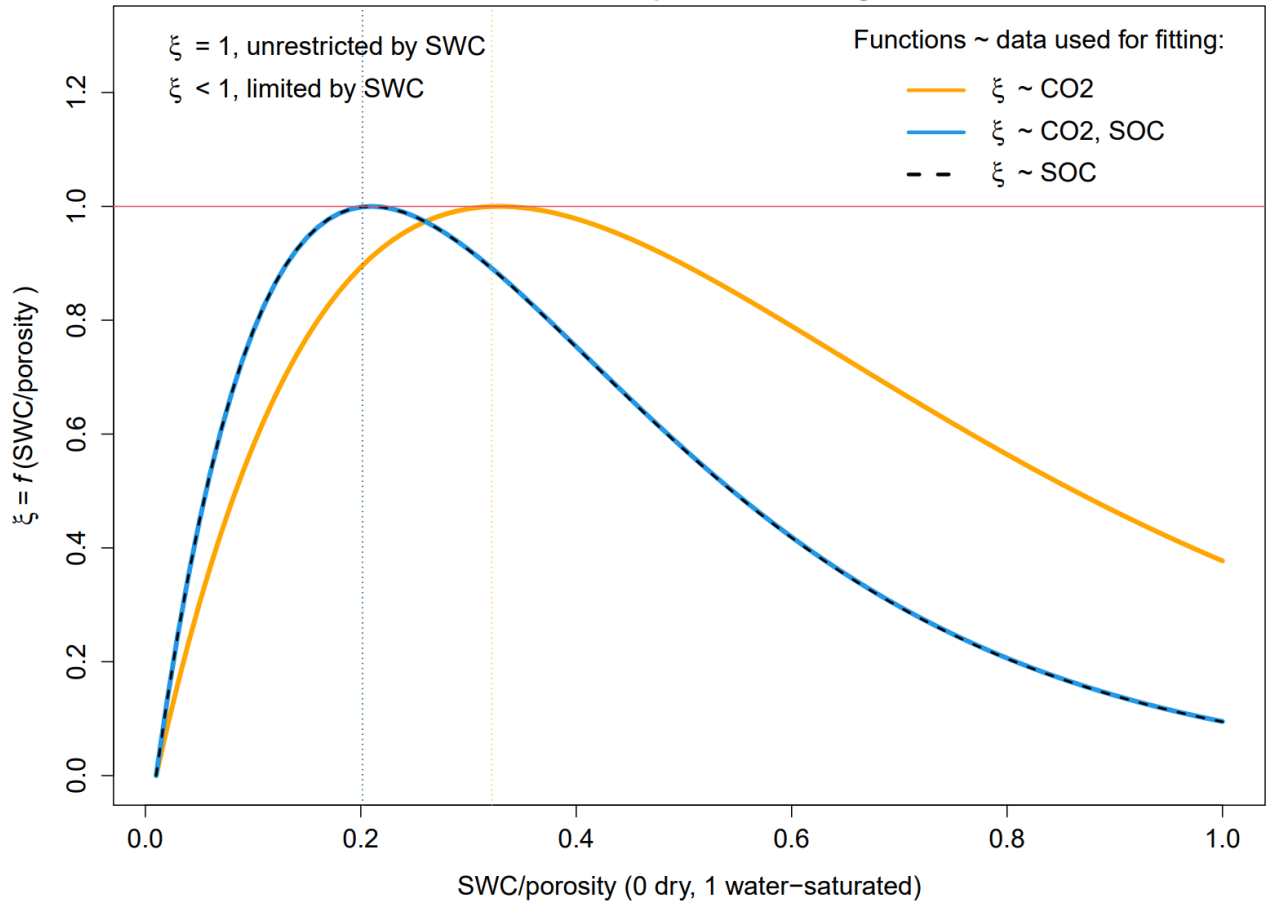
1 Introduction

Soil moisture and soil C stocks in boreal forests are higher in forested peatlands on frequently paludified organo-mineral soils and peatlands on water-saturated organic soils than in well-drained forests on mineral soils (Weishampel et al., 2009; Ťupek et al., 2008; Bhatti et al., 2006; Hartshorn et al., 2003). Almost a quarter of the total terrestrial C (440 Pg C) stored in boreal moist and dry soils has accumulated since the last glaciation (Scharlemann et al., 2014) and is expected to create large C losses under warming climates (Hararuk et al., 2015). Moist organic soils are crucial for modelling dynamics of the global C cycle as they store five times more carbon than dry mineral soils (Leifeld and Menichetti 2018; Turetsky et al., 2015; Scharlemann et al., 2014). However, soil organic carbon (SOC) stocks modelled by Earth System models (ESM) show large uncertainty due to structural model differences (Hashimoto et al., 2017; Hararuk et al., 2014, 2015; Todd-Brown et al., 2013), and differences in environmental drivers and their functional dependencies used by soil C models (Thum et al., 2020; Ťupek et al., 2019; Falloon et al., 2011).

Despite soil moisture being a dominant driver of variation in C dynamics (Humphrey et al., 2022), ESMs lack consensus on the response of decomposition to soil moisture and temperature (Yan et al., 2018; Sierra et al., 2015; Falloon et al., 2011). The functional forms of the temperature and moisture modifiers of default decomposition rates among models disagree in their representation of extreme cold/dry and hot/wet conditions (Sierra et al., 2015). For example, the moisture decomposition dependency in the Yasso07 soil C model (Tuomi et al., 2011, 2009) is based on annual precipitation, has a functional form reaching saturation, and is uninformed about soil characteristics. The use of the saturation function is limited to well drained soils as under wet or poorly drained forest soils such model results to underestimation of the C stocks (Dalsgaard et al., 2016, Ťupek et al., 2016). The soil module of the CENTURY model (Adair et al., 2008; Parton et al., 1996; Metherall et al., 1993) uses precipitation and basic soil data (bulk density, clay, and silt contents) to calculate soil moisture, which similarly to Yasso07 assumes saturation of decomposition rates. Other functional dependencies of moisture such as DAYCENT, Demeter, Standcarb, Candy, Gompertz, Mayers, Moyano, and Skopp assume all kinds of functional forms (e.g., Gaussian increase with optimum and reduction of decomposition, continuous linear increase or with saturation, linear increase until optimum and linear reduction) (Kelly et al., 2000; Foley, 2011; Harmon and Domingo, 2001; Bauer et al., 2008; Janssens et al., 2003; Mayers et al., 1982; Moyano et al., 2013; and Skopp et al., 1990 as cited by Sierra et al., 2015). The wide variation in commonly used moisture functions may result from the variety of data from different soil types and climates used to constrain these moisture indices.

If environmental response functions were calibrated for mineral soils only, then these functions may not adequately represent responses in the moisture range characteristic of organic soils. For example, default response functions of soil C models cannot represent anoxic inhibition of decomposition rates in paludified peatland forest soils. However, the inhibition of decomposition can be accounted for by a reduction parameter such as "anerb" in CENTURY (Metherall et al., 1993). Due to variable water level and its determination of soil oxic/anoxic conditions and SOC accumulation in peatlands, peat SOC stocks are typically modelled with models specifically developed for peatlands (Bona et al., 2020; Kleinen et al., 2012; St-Hilaire et al., 2010;

Frolking et al., 2010, 2001; Clymo 1992). However, for global applications on peatlands, the general soil models in ESMs can be modified for peat soil by adjusting parameters such as the hydraulic conductivity, as seen in models like JULES (Chadburn et al., 2022) and ORCHIDEE (Qiu et al., 2018), or by reducing decomposition rates for wetlands as in LPJ (Wania et al., 2010) and JSBACH (Goll et al., 2015). The land surface model JSBACH coupled with the Yasso soil C model adopts heuristic 65% reduction of decomposition for wetlands (Kleinen et al., 2021; Goll et al., 2015). Using CENTURY model at the site-level, Raich et al. (2000) opted for improvement in modelled SOC of wetlands by modifying the environmental function for sites with insufficient drainage. This approach improved CENTURY compared to default Yasso07 in poorly drained forested peatlands in Sweden, though the SOC stocks of both models were still underestimated (on average by 10 and 13 kg C m^{-2}, respectively) (Ťupek et al., 2016). Similar magnitude of SOC underestimation of Yasso07 model with default dependency on precipitation was also observed for poorly drained forest soils (e.g., gleysols and organic soils) in Norway (Dalsgaard et al., 2016).

We hypothesised that the SOC stocks and CO_2 emissions of mineral and organic (peat) soils can be modelled accurately by revising the original precipitation-based environmental modifier of a parsimonious model like Yasso07 with a function accounting for the reduction of decomposition based on the long-term near surface moisture. Near surface moisture is strongly correlated with the ground water level depth in peatlands (Dimitrov et al., 2022) and the moisture values between mineral soil forests and peatlands are comparable on the same scale, which makes soil water content (SWC) a suitable variable for representing landscape moisture variation. Boreal forest SWC can either be measured in-situ or derived in high resolution using hydrological models (e.g., Leppä et al., 2020; Launiainen et al., 2019) and at larger scale by remote sensing and machine learning (Han et al., 2023). We aimed to develop the original Yasso07 model with global parameters as in Tuomi et al. (2011) by adding a revised unimodal moisture-based environmental function. We then optimized this function using Bayesian data assimilation of measurements from a boreal forest-mire hillslope catena of mineral, organo-mineral, and organic soils, and tested whether we could correctly reconstruct observed SOC stocks and CO_2 emissions.

2   Methods

2.1   Study sites

Nine forest/mire site types in this study were situated along the hillslope from Vatiharju esker to Lakkasuo mire in southern Finland (61º 47', 24º 19') (Fig. 1) and formed a forest-mire ecotone, a gradient in soil moisture and nutrient status, vegetation composition, biomass production, and SOC stocks (Dimitrov et al., 2014). The sites were situated along a 450 m transect on a 3.3 % slope facing NE with a relative relief of 15 meters. The site typology described below was based on the vegetation composition reflecting site wetness, fertility, and location on the slope according to Finnish forest and mire classification systems (Cajander 1949; Laine et al., 2004).

120 On the crest of the esker was a well-drained xeric Scots pine forest (CT – Calluna type) which changed down the slope to subxeric mixed Scots pine - Norway spruce forest (VT – Vitis-idaea type), and in mid-slope to mesic and herbrich Norway spruce dominated forest (MT – Myrtillus type, OMT - Oxalis-myrtillus type) together referred to as mineral soils upland forests. On the toe of the slope were forest-mire transitions on gleyic organo-mineral soils or mixed spruce pine birch forests (OMT+ - Oxalis-myrtillus Paludified type, KgK – Myrtillus Spruce Forest Paludified type, and KR – Spruce Pine Swamp

125 type). On the level were water-saturated sparsely forested mires on histosols (VSR1 and VSR2 - Tall Sedge Pine Fen types).

The understory or forest floor vegetation along the ecotone changed from being dominated by *Calluna* and *Vaccinium Vitis-idaea* dwarf-shrubs and typical forest mosses on the uppermost sites (CT, VT), to *Vaccinium myrtillus* dwarf-shrubs with herbs in the mid-slope (MT, OMT), *Vaccinium myrtillus* dwarf-shrubs with herbs and *Sphagnum* in the transitions (OMT+, KgK, KR), and *Vaccinium oxycocus* and *Betula nana* dwarf-shrubs with *Menyanthes triofoliata, Carex* and *Sphagnum* species on

130 the level (VSR1, VSR2) (Fig. 1). More detailed tree stand, soil and climate characteristics for these sites were reported by Ťupek et al. (2008, 2015).

2.2   Auxiliary measurements

Soil temperature, water content, and CO_2 emissions (gCO_2 m^{-2} h^{-1}) were measured simultaneously during years 2004, 2005, and 2006. The measurement campaigns were conducted in one or two days between 7 am and 6 pm weekly during the

135 vegetative season of 2004 (July-November), 2005 (May-November), 2006 (May-September), and monthly during the non-vegetative season (December-April). The summer seasons of the years 2004, 2005, and 2006 showed exceptionally different monthly weather patterns. Data from Finnish meteorological station, located 3 km north-east from the ecotone in Juupajoki, showed that the summer season in 2004 was rainy and colder in comparison to long-term typically mild weather, in 2005 weather was typical, and in summer 2006 the weather was sunny and warm. The exceptional drought in 2006 caused by the

140 lack of rain and increased temperatures in June and later July – early August (Gao et al., 2017) caused visible drying of the moss layer along all the sites of the ecotone. The 2006 summer drought ended with showers in mid-August and with more frequent rain in autumn the soil moisture recovered to a normal level.

2.2.1   Soil temperature and moisture conditions

The soil temperature was measured at depths of 5 cm (T_5, °C) with a portable thermometer, and the soil volumetric water

145 content at depth of 10 cm (SWC_{10}, %, m^3 m^{-3}) in all sites with a portable ThetaProbe (Delta-T Devices Ltd) calibrated for each site type. The SWC calibration accounted for the bulk density/porosity of forest type specific soils (Ťupek et al., 2008, 2015). Because the forest-mire variation of soil organic layer bulk density was relatively small 0.34+/-0.07 g cm^{-3} (porosity 74+/-5%) (Ťupek et al., 2015) the values SWC of top 10 cm were in the same order of magnitude between the forest/mire site types. For missing field campaigns during months with the snow cover (Nov 2004, Feb – Apr 2005, Dec 2005 – Apr 2006) we

150 interpolated the measured monthly mean T_5 and SWC_{10} time series with a spline function. The SWC_{10} values among the forest

and mire site types ranged between 0 and 1 (or 0 and 100 %) (Figure 3), whereas in comparison to water level depth the values range from 8 cm in tall-sedge mire to 881 cm in pine forest on the top of the esker (Tupek et al. 2008).

2.2.2 Soil CO₂ emissions

Measurements of forest soil heterotrophic respiration (R_h, gCO_2 m^{-2} h^{-1}, positive sign) were taken using opaque cylindrical chambers (30 cm diameter, 21.2 L) placed on metallic collars (30 cm in diameter) which were installed permanently into 30 cm soil depth. The collars locations (3 for each site type, 12 for mineral soil forests, 9 for transitions, and 6 for mires, together 27) were selected to represent the spatial variation of each site type and the spatial variation along the forest-mire ecotone (e.g., dominant forest floor vegetation, microtopography, soil drainage, and nutrient status).

The aboveground forest floor vegetation inside each collar was clipped at the time of collars installation and any plant regrowth of e.g., mosses was clipped approximately half an hour before the flux measurements. At the time of the collar installation the roots of the understory vegetation and trees were cut with a saw along the collars' perimeter. The metallic collars installed to 30 cm soil depth prevented the regrowth of the roots. Due to the vast majority of tree and understory roots in boreal forest occurring in the humus layer, the 30 cm depth was considered sufficient to cut the roots thus remove the signal of the root autotrophic respiration from the net CO_2 emissions. In transitions and mires the depth of peat could be more than 30 cm (in range from 0.15 m in OMT+ to 1.2 m in VSR2 (Ťupek et al., 2008)) but the prevailing high ground water levels (in range from 33 cm in OMT+ to 7 cm in VSR1 (Ťupek et al., 2008)) limit the root growth into the upper/sub-surface layer.

The soil CO_2 emissions were measured every 4.8 s during 80 s intervals with a portable infrared CO_2 analyser (EGM4, SRC-1 PP systems Inc.). We calculated CO_2 flux rates from the development of CO_2 concentration over time inside the chamber.

2.2.3 Soil organic carbon stocks

The soil data from the 2006 sampling up to 30 cm depth (Ťupek et al., 2015) were combined with additional soil sampling cores of up to 100 cm depth in October 2015 (3 per site) (Fig. S1). The bulk density, C and N concentrations for new samples were determined as in Ťupek et al. (2015).

The SOC content (g cm^{-3}) of separate soil layers were interpolated for the whole profile with the fitted spline functions and summed up for each depth and each forest/mire site (Fig. S1). The SOC content was similar in the upper-most humus layers of all forest/mire types (below 0.3 g cm^{-3} in a layer 0-10 cm), but in the sub-surface level (10-30 cm) clearly doubled from uplands to transitions and mires (from below 0.2 to above 0.4 g cm^{-3}) (Fig. S1). In the soil layers below 30 cm the SOC content showed differences in degrees of magnitude (around 0, 0.01, and 0.1 g cm^{-3} for forests, transitions, and mires, respectively) (Fig. S1). The SOC stock (kg C m^{-2}) was a result of SOC content multiplied by a bulk density.

180 **2.2.4 Biomass of tree stand and understory vegetation**

Breast height diameter and height of all Scots pine (*Pinus sylvestris*), Norway spruce (*Picea abies*), and Silver birch (*Betula pendula*) trees on each forest site type were measured in 2006. The biomass components for each species (leaves, branches, stems, coarse-roots) were estimated with biomass conversion functions (Repola et al., 2008, 2009) and fine-roots with functions by Lehtonen et al. (2015). Forest floor plants from three 0.07 m^2 sample plots located nearby soil respiration

185 measuring collars were harvested for each forest/mire site type in June-July 2004 (Ťupek et al., 2008). Plants were separated to herbs, mosses, and shrubs, dried and weighed for each category and each sample plot. The stand density and the tree biomass increased from xeric (CT) and mesic upland forest sites (VT and MT) towards the herb-rich forest site (OMT) and transitions (OMT+, KgK, and KR), and decreased to very sparse canopy in peatlands/mires (VSR sites) (Fig. 1b). The understory aboveground biomass correlated negatively with the density of the canopy cover thus positively with the light intercepted onto

190 the forest floor (Ťupek et al., 2008).

2.3 Data analysis

2.3.1 Yasso07 SOC and CO_2 modelling

Equilibrium SOC stocks of up to 1 m depth, SOC changes and soil CO_2 emissions (Rh) for the forest/mire types were modelled using the Yasso07 soil carbon model (Tuomi et al., 2009, 2011) with specific litter input and weather data in accordance with

195 the method of Finnish greenhouse gas inventory (Statistics Finland, 2023). The temperature and precipitation data for the weather input was from the nearest Finnish meteorological institute (FMI) weather station located 3 km away from our study sites. We first ran the Yasso07 model using the original formulation of the environmental function with precipitation and air temperature data, and then we ran the Yasso07 model fitted with the environmental modifier function based on SWC_{10} and T_5 of the forest/mire site types using the Bayesian data assimilation technique.

200 **2.3.1.1 Yasso07 soil C model**

The Yasso07 is a semi-empirical process-based soil carbon model where soil C is divided based on the organic matter solubility into five pools (C_A, C_W, C_E, C_N, and C_H) from which three are fast (acid- (A), water- (W), and ethanol- (E) soluble), one is slow (non-soluble (N)) and one is almost stable (humus (H)) (Tuomi et al., 2011). The rates of C decomposition in each pool and C transfers between the pools are affected by climate. The model can be expressed mathematically as a set of differential

205 equations where decomposition of the entire structural matrix of C pools $C_A…C_H$ defined by default mass flow parameters $\alpha_{A,W}…\alpha_H$ and decomposition coefficients $k_A…k_H$ (A_{YS}) is scaled by the time step dependent scalar of the environmental rate modifier $\xi(t)$ Eq. (1).

$$
\frac{dc(t)}{dt} = \begin{pmatrix} i_A \\ i_W \\ i_E \\ i_N \\ i_H \end{pmatrix}(t) + \xi(t) \begin{pmatrix} -k_A & \alpha_{A,W}k_W & \alpha_{A,E}k_E & \alpha_{A,N}k_N & 0 \\ \alpha_{W,A}k_A & -k_W & \alpha_{W,E}k_E & \alpha_{W,N}k_N & 0 \\ \alpha_{E,A}k_A & \alpha_{E,W}k_W & -k_E & \alpha_{E,N}k_N & 0 \\ \alpha_{N,A}k_A & \alpha_{N,W}k_W & \alpha_{N,E}k_E & -k_N & 0 \\ \alpha_H k_A & \alpha_H k_W & \alpha_H k_E & \alpha_H k_N & -k_H \end{pmatrix} \begin{pmatrix} c_A \\ c_W \\ c_E \\ c_N \\ c_H \end{pmatrix}(t) \tag{1}
$$

Where t is time, i defines a vector of initial carbon pools $i_A \dots i_H$, and subscripts in α indicate mass transfer pools (e.g., $\alpha_{A,W}$ defines mass transfer from pool W to pool A). The total soil respiration or CO_2 efflux (Rh) is a product of a column vector by a row vector C(t), where the elements of the column vector are the fractions that were not transferred among the pools (Sierra et al. 2012).

The model was originally calibrated for running on annual time steps (Tuomi et al., 2009), but it can run on monthly steps with monthly decomposition rates (1/12 of annual $k_A \dots k_H$), and monthly litter and climate data (Ťupek et al., 2019). Then $\xi(t_m)$ is defined by a combined function of monthly air temperature (T_m) and 1/12 of annual precipitation ($P_a/12$) (Eq. (2)).

$$\xi_T(t_m) = e^{(\beta_1 T_m + \beta_2 T_m{}^2)}\left(1 - e^{\gamma\frac{P_a}{12}}\right) \tag{2}$$

Where β_1, β_2, and γ are parameters of the environmental function and t_m is the monthly time step. To test our hypothesis of running the model for a catena of soils with gradually increasing moisture content (from xeric to mesic, paludified, and saturated), we re-defined the $\xi(t_m)$ function for the use with soil temperature based on a Q_{10} exponential function to T_5, and moisture data using adjusted hump shaped Ricker function (Bolker, 2008) for response to SWC_{10} which limits decomposition rate outside the optimum soil water content (ξ_{AR}, Eq. (3)).

$$\xi_{AR}(t_m) = Q_{10}^{(\frac{T_5 - 10}{10})} a SWC_{10} e^{(-ae^{-1}SWC_{10})} \tag{3}$$

Where the Q_{10} parameter represents the increase of the temperature function over 10 °C difference in T_5, and the *a* controls both ascending and descending slopes of the moisture function when the peak is set to 1. In the Ricker function with a and b parameters and an independent variable vector x (axe^{-bx}), the height of the peak can be inferred as $(a/b)e^{-1}$, and the x value of the peaks location as 1/b (Bolker, 2008). Thus, in our formulation by setting the peak in the Ricker function to 1 we could substitute b parameter by ae^{-1} and the SWC_{10} optimum (the SWC_{10} when decomposition is at optimum) was inferred as $1/ae^{-1}$.

The Yasso07 model versions in this study run accordingly:

1. the Yasso07.ξ_{TW} version is the Yasso07 coupled with original ξ_T (Eq. (2)) and with the original global parameter set (Tuomi et al., 2011) but with two k-rates parameter sets, (i) the original $k_A \dots k_H$ rates for application on mineral soils applied for mineral and organo-mineral soil forests (CT, VT, MT, OMT, OMT+, KgK, KR) and (ii) with an inhibitor reducing k-rates by 35% ($0.65k_A \dots 0.65k_H$) for application on wetlands (Goll et al., 2015, Kleinen et al., 2021) applied for mire sites (VSR1 and VSR2);

2. the Yasso07.ξ_W wetland version is the same as the Yasso07.ξ_{TW} but with a fine-tuned k-rates inhibitor to fit the SOC of mire sites (VSR1 and VSR2);

3. the Yasso07.ξ_{AR} version for soil moisture gradient from mineral to peat soils (e.g., as in boreal forest - mire ecotone) is the Yasso07 model coupled with ξ_{AR} (Eq. (3)) with the original global parameter set of the structural matrix and optimized parameters of ξ_{AR}.

240 The initial equilibrium SOC stock (C_o) for each forest/mire type for the pre-trenching period was simulated analytically (Xia et al., 2012) (Eq. (4)).

$$C_o = -\xi A_{YS}^{-1}\bar{u} \qquad\qquad\qquad\qquad (4)$$

Where ξ is the environmental modifier, A_{YS} is a structural matrix formulation of Yasso07 model's differential equations, and $\bar{u}$ is the litter input (mean annual litter of foliage, branches, stem, stump, roots, and understory).

245 The Yasso07 model source code, used here, was built in R software (R Core Team 2023) on the platform of the SoilR package (Sierra et al., 2012) according to the mathematical description and parameters of Tuomi et al. (2011). The model outputs are monthly SOC stocks and soil CO_2 emissions. The model was run with data inputs of above- and below-ground litterfall (accounting for its chemical composition) and climate data (described in more detail below). Monthly model outputs of heterotrophic soil respiration were compared to mean monthly Rh measurements.

250 **2.3.1.2   Climate and litter C input data for Yasso07 model**

The Yasso07.ξ_{TW} was run with monthly air temperature and precipitation from the nearby Juupajoki weather station of the Finnish meteorological institute. The Yasso07.ξ_D was run using site type specific continuous monthly T_5 and SWC_{10} time series.

The litter C input of the forest/mire types (Fig. S2 and Fig. S3) used by Yasso07 was estimated as in Lehtonen et al. (2016) 255 based on turnover rates of tree stand biomass components (including fine- and coarse-roots, stump, branches, and foliage) and understory vegetation. The litter C input was separated into Yasso07 A, W, E, N pools according to the component and species (or species groups) specific A, W, E, N ratios taken from the literature (Berg et al., 1991a, 1991b, 1993; Gholz et al., 2000; Trofymow et al., 1998; Vávřová et al., 2009; Straková et al., 2010) (Table S2). The annual litter was distributed to monthly resolution by accounting for seasonal trends of foliage, fine-roots, and understory (Ťupek et al., 2019; Zhiyanski 2014) or 260 evenly. The litter input before trenching was assumed to represent the long-term average of the equilibrium state forest (Fig. S2a, Fig. S3). During trenching the severed fine- and coarse-roots made up the major component of the total litter (Fig. S2b) and resulted in a clear peak in the monthly litterfall time series (Fig. S3). After trenching the monthly litter levels decreased as the sum of components excluded the roots (Fig. S2c, Fig. S3).

2.3.1.3   Bayesian SOC and CO_2 data assimilation

265 The Bayesian posterior uncertainty provides updated information on parameter values based on pre-existing information on the parameters and the data through the likelihood function (Speich et al., 2021). The d, Q_{10}, and SWC_{opt} parameters of the ξ_D (Eq. (4)) coupled with Yasso07 model were optimized on the level of the forest-mire ecotone using Bayesian data assimilation

technique (Luo et al., 2011; Hartig et al., 2012; Speich et al., 2021) with observed SOC stocks and monthly Rh data of forest/mire types with prior information on best parameter values obtained from a purely empirical NLS model (Table 1) and the defined parameter range in Table S1. During the optimization, the Yasso07.ξ_D model was first run only with observed SOC stocks and second with both SOC stocks and Rh data combined obtaining a probability distribution of model parameters of ξ_D (the posterior uncertainty $p(\theta|y)$ conditional on the observations (y) and prior knowledge on the parameter values $p(\theta)$). The sum of the probability density for the target parameter set (θ) between the model predictions and observations was maximized for the best agreement using the likelihood defined by a modified Laplace probability density function $p(y|\theta)$ (the probability of observing the data y with the model parameters set θ) where we allowed the width of the distribution to be affected by the observed SOC and Rh values (Eq. (5)).

$$p(y \mid \theta) = \prod_{j=1}^{2} \prod_{i=1}^{N_j} \frac{1}{2(a_j+b_j x_{j,i})} \; e^{\frac{-\left|(x_{j,i}-\mu_{j,i})\right|}{a_j+b_j x_{j,i}}} \tag{5}$$

where $\mu_{j,i}$ is the observed j^{th} variable (e.g., SOC, CO_2, or SOC and CO_2) of ith observations, x_i is the modelled prediction, N is the total number of observations, and a, b are parameters affecting the width of the distribution. In the combined SOC and CO_2 likelihood, the likelihood function $p(y \mid \theta)$ was then the multiplication of the distributions of SOC and CO_2 at all observation times. We evaluated the variation in the estimated parameters by separating data for fitting the models and testing with 9-fold cross validation technique.

The model parameters of ξ_D and $p(y|\theta)$ were sampled from an assumed uniform distribution within their prior ranges (Table S1). Posterior probability distributions of parameters (Table 2) were derived by using the differential evolution (DEzs) Markov Chain Monte Carlo (MCMC) sampler (ter Braak and Vrugt, 2008) with the runMCMC function from the BayesianTools package in R (Hartig et al., 2012) and by computing three chains in parallel. The convergence of MCMC runs was evaluated using Gelman–Rubin multivariate potential scale reduction factor (psrf) (Brooks and Gelman, 1998). The MCMC simulation was considered converged if psrf was below 1.05 for all parameters (1.028 and 1.048 for $p(\theta|SOC)$ and $p(\theta|SOC\text{-}CO2)$, respectively). Trace plots of MCMC runs for target parameters showed effective sampling and unimodal parameter density with clearly defined peaks. The differences in parameter uncertainties (difference between 97.5% and 2.5% quantiles of the 95% confidence interval) were not significant ($p = 0.99$) when evaluated with a Welch Two Sample t-test between two posterior distributions $p(\theta|SOC)$ and $p(\theta|SOC\text{-}CO2)$ (Table 2).

2.3.1.4 Performance evaluation of Yasso07.ξ_{TW} and Yasso07.ξ_D

The performance of Yasso07 model versions (i) Yasso07.ξ_{TW} and (ii) Yasso07.ξ_D with ξ_D parameter set θ from two posterior distributions, $p(\theta|SOC)$ and $p(\theta|SOC\text{-}CO_2)$, was evaluated with the modelled SOC and CO_2 outputs against the observed data in the forest mire-ecotone with the coefficient of determination (R^2), the mean absolute error (MAE), mean bias error (MBE), the root-mean-square error (RMSE), the Akaike information criterion (AIC) for considering the number of model parameters

in the error calculation as in Abramoff et al. (2022), and the fitted linear trends of normalized SOC and CO_2 model residuals with observations against T_5 and SWC_{10} data.

3   RESULTS

3.1   Distributions of SOC stocks and Rh in relation to SWC

The SOC stock measurements (to a depth of 1 m) in forest-mire ecotone were distributed in range between 20 in well-drained soils of upland forests and 125 kg C m^{-2} in poorly drained soils in peatlands/mires (Fig. 2). The SOC stock values strongly correlated with the long-term moisture levels. The median Rh values ranged between 0.4 and 0.6 gCO_2 m^{-2} h^{-1} for upland forests, 0.4 and 0.5 gCO_2 m^{-2} h^{-1} for forest-mire transitions, and 0.3 and 0.4 gCO_2 m^{-2} h^{-1} for mires (Fig. 2). The forest/mire site type differences in median Rh values expressed per m^2 were small and poorly correlated with the mean soil moisture levels.

3.2   Distribution of Rh in climate space of soil T and SWC

The site-specific time series of hourly R_h measured in the forest/mire ecotone during years 2004, 2005, and 2006 followed a typical seasonal pattern of temperature and was distributed in range between 0.08 and 1.6 gCO_2 m^{-2} h^{-1} depending on the corresponding soil temperature and moisture conditions (Fig. 3). The Rh values were generally larger during wet years than during a typical year, and lowest during dry years (Fig. 3).

The T_5 and SWC_{10} values showed a typical seasonal variation (in range between around 0 and 20°C, dryest in summer and wettest in late autumn/spring) (Fig. 2b and 3c). The T_5 showed similar magnitude among the forest/mire sites, whereas the SWC_{10} increased from driest (upland forest) to intermediate (forest-mire transition), and from upland to lowland for the wettest (mire) sites located on the slope (Fig. 3). The volumetric SWC_{10} (%) were comparable in the same order of magnitude between the forest/mire site types because the forest-mire variation of the soil organic layer bulk density was relatively small 0.34+/-0.07 g cm^{-3} (porosity 74+/-5%). The forest-mire ecotone soil moisture at 10 cm depth ranged from 5% to 91%. The minimum, maximum and mean SWC at 10 cm depth between forests, transitions, and mires clearly differed showing the gradient of increasing moisture from forests to mires (Fig. 2a, Fig. 3). Due to highly variable weather (wet, typical, and dry year) all ecosystems experienced periods of extremely low and high SWC_{10} values. The SWC_{10} of upland forest ranged between 5 and 25%, between 17 and 70% in transitions and mires between 49 and 91% (Fig. 3). The variation of soil temperature at 5 cm depth along the ecotone was similar among the forest/mire types and ranged between -3 and 22 °C (Fig. 3). The R_h values during dry 2006 year were in comparison to previous years clearly reduced mostly in upland forest and forest-mire transitions (Fig. 3). The spatial soil moisture gradient of forest/mire types was not clearly reflected in distribution of Rh values when expressed in gCO_2 m^{-2} h^{-1} (Fig. 2) (unless expressed as a C fraction of SOC). The short-term SWC variation impacted the typical seasonal levels of Rh values mainly during the extreme events (rainy summer period in wet years, or drought summer period in dry years) (Fig. 3).

3.3 ξ_{AR} optimized with Yasso07.ξ_{AR}

The optimization of ξ_{AR} (Eq. (3)) coupled with Yasso07 showed that in the catena of mineral and organic soils of the boreal forest-mire the optimum moisture content for decomposition and CO_2 emissions was in well drained mineral soil forests (SWC_{opt} medians between 14 and 27%, Table 1, Fig. 4). The MCMC fit with CO_2 data produced larger SWC_{opt} and larger tail in the Ricker function (compared to SOC or SOCCO2 fit). The decomposition rate outside the moisture optimum reduced decomposition similarly for the two data sources (SOC and SOC-CO_2) used for calibration. However, the temperature and moisture functions were different when only CO_2 was used for calibration.

The two SOC and SOCCO2 based Q_{10} functions showed a similar increase with T_5 until 10 °C (Fig. 4a). Similar patterns were observed for ξ_{AR} in the climate space of T_5 and SWC_{10} (Fig. 5a and b). The stronger temperature sensitivity of $\xi_{AR,p(\theta|CO2)}$ with median Q_{10} value 4.5 resulted in a more pronounced increase in decomposition rates especially in climate space with high water saturation (Fig. 4 and Fig. 5c). The SOC and SOC-CO_2 based $\xi_{AR}Q_{10}$ values for the forest – mire ecotone (medians 2.3 or 2.5, Table 1) were lower.

3.4   Performance of Yasso07.ξ_{TW}, Yasso07.ξ_W and Yasso07.ξ_D

The model performance evaluation showed that the soil water and temperature modifier ξ_D coupled with Yasso07 model (Yasso07.ξ_D) outperformed the original Yasso07 environmental function even after 65 % reduction of decomposition rates for wetlands was applied (Yasso07.ξ_{TW}) (Table 2, Fig. 5). Although, the Yasso07.ξ_{TW} model version accurately predicted SOC stocks of mineral soil forests (CT…OMT), it heavily underestimated the SOC stocks of organo-mineral forested peatlands and mires (OMT+…VSR2), thus it showed the most biased model performance metrics (highest RMSE, MBE, MAE, AIC and lowest R^2_{adj}) among the model versions compared (Table 2). Reduction of decomposition rates of 65% for mires in Yasso07.ξ_{TW} was not sufficient to simulate their SOC stocks as simulated SOC of mires were only about 10 % of measured values (Figs 5a, 5b, and 5c). The SOC simulations for VSR mires with Yasso07.ξ_W would have required as much as a 96% reduction of the decomposition rates. The optimized Yasso07.ξ_{AR} model version accurately simulated SOC stocks throughout the forest – mire ecotone.

The version Yasso07.$\xi_{AR,p(\theta|SOC)}$ outperformed Yasso07.$\xi_{AR,p(\theta|SOC-CO2)}$ when evaluated against SOC data and both models were similar when evaluated against CO_2 data (Table 3, Fig. 5). The Yasso07.$\xi_{AR,p(\theta|CO2)}$ outperformed the functions based on SOC or SOCCO2 against measured CO_2 data but failed when evaluated against measured SOCs. The Ricker function improved the representation of decomposition for drier soils and the representation of optimal SWC for decomposition.

The SWC optimum was derived from the fitted ascending slope parameter and its values were between 14 and 27 % (depending on the data used for fitting; 14% for SOC and CO_2 and 27% for CO_2). The MCMC fit with CO2 data produced larger SWCopt and larger tail in the Ricker function (compared to SOC or SOC CO_2 fit). However, the CO_2 only fit also underestimated SOC stocks of forested peatlands (Fig. 5a). The normalized SOC residuals of the two Yasso07.ξ_{AR} models based on SOC or SOC

and CO_2 did not show any large T_5 or SWC_{10} trends (Figs 5a, 5b, and 5c). Although, measured Rh fluxes during the cold season may be slightly overestimated.

The soil CO_2 emissions simulated with the original Yasso07.ξ_{TW} agreed unexpectedly well with observed Rh values (Table 2, Figs. 6d, 6e and 6f) outperforming the Yasso07.$\xi_{AR, p (\theta | SOC)}$ version (Table 2, Fig 6e). On the other hand, the Rh simulated with Yasso07.$\xi_{AR, p (\theta | SOC)}$ performed similarly as Yasso07.ξ_{TW} in terms of RMSE (same RMSE 0.16 g CO_2 m^{-2} hour^{-1} for both models). The performance statistics for Yasso07.ξ_{AR} based on SOC and SOCCO2 were better compared with Yasso07.ξ_{TW} for SOC and about the same for Rh (Table 2). The performance statistics for Yasso07.ξ_{AR} based on CO_2 were best among the models for CO_2 but fail in similar fashion for SOCs as Yasso07.ξ_{TW}. The normalized modelled residuals showed that both Yasso07 model versions (Yasso07.ξ_{TW} and Yasso07.$\xi_{AR, p (\theta | SOC)}$) showed small Rh biases in extreme, very cold and in very warm temperatures (Fig. 6e). The normalized CO_2 residuals of the Yasso07.$\xi_{AR, p (\theta | CO2)}$ showed no bias among the functions (0 MBE, Table 2). The normalized CO_2 residuals evaluated against with SWC_{10} did not show any bias for any of the models (Fig. 6f).

4   Discussion

The Yasso07 model (Tuomi et al., 2011) coupled with a revised and optimized empirical Q_{10} soil temperature and Ricker moisture function ξ_{AR} (Eq. (3), Fig. 4), successfully reconstructed observed variation of SOC stocks and soil heterotrophic CO_2 emissions with increasing soil wetness in mineral, organo-mineral, and peat soils in boreal forest (Fig. 6). The Bayesian MCMC data assimilation has proven useful also in other studies (e.g., Xu et al., 2006; Hararuk et al., 2014).

Our application of Yasso07 models on the hillslope accounted for the continuity in moisture conditions which was reflected in the modelled gradient of mineral and peat soils carbon stocks. The Yasso07 model initially developed for mineral soils was improved for application in peatlands by accounting for the soil temperature and volumetric moisture, as these are better predictors of heterotrophic respiration than air temperature and precipitation (Jian et al., 2022). Although, the empirical Ricker function ξ_{AR} used here was heuristic, its form implicitly accounted for prevailing intrinsic micro-scale processes on the hillslope controlling Rh and SOC accumulation e.g., plant and microbial communities, long-term and short-term limitation of oxygen and substrate with moisture (Davidson et al., 2012, Moyano et al. 2012, Ghezzehei et al. 2019).

The ξ_{AR} being able to simulate gradually increasing SOC stocks from mineral to organic soils makes it a preferable rate modifier for the Yasso07 model, instead of simply adjusting decomposition with a reduction constant for wetlands (e.g., Goll et al., 2015; Kleinen et al., 2021), which underestimated the SOC stocks of peatlands (Yasso07.ξ_{TW} in Fig. 5). In this study, the constant 96% reduction (0.04*k-rates) was proposed for the existing Yasso07.ξ_{TW} for more accurate SOC modelling in mires, a value comparable to rates of anaerobic decomposition (Schuur et al., 2015). Currently, 80% reduction of rates is used for water-saturation in an updated moisture modifier in the JULES model (Chadburn et al., 2022). Although JULES reduces

decomposition linearly from the maximum rate 1 at the moisture optimum (30% - 75% SWC) to a reduced rate 0.2 in water-saturated peat soils.

4.1 The moisture response

The use of gradually changing near surface soil moisture avoids biases in land surface modelling related to ignoring high SOC stocks of organo-mineral soils of forested peatlands (Dalsgaard et al., 2016, Ťupek et al., 2016), e.g., forest-mire transitions (Fig. 1, and Fig. 2). The modelling decomposition rates accurately with diffusion-based moisture functions accounting for microbial processes requires correct representation of the drivers of heterotrophic respiration (Yan et al., 2018; Moyano et al., 2012, 2013; Manzoni et al., 2012; Ghezzehei et al., 2019). However, uncertainty in functional moisture - soil respiration dependencies are high (Sierra et al., 2015; Falloon et al., 2011) and dependencies vary with the soil properties, e.g., SWC optimum increases for soils with higher organic C content (from 30% to 75% SWC, Moyano et al., 2012, 2013). The moisture optimum found in soil respiration datasets of sites from a larger moisture range was found in 50% water-filled pore space (WFPS) and corresponding to around 31% SWC assuming mean porosity of 62%, Hashimoto et al., 2011). Our SWC_{opt} between 14 and 27% SWC (Table 1) was somewhat lower than in other studies.

In its impact on decomposition of the ξ_{AR} functions (calibrated with SOC, SOCCO2, and CO2 data) incorporated into Yasso07 soil C model were comparable (e.g., all found the moisture optimum in dry soils of forest-mire ecotone). Although, the soil temperature and moisture function showed a relatively small differences in Q_{10}, the a parameter of CO2 based fit was larger than from SOC and SCOCO2 fit (Table 1). In terms of the Yasso07 model constants, if temperature and moisture conditions are favourable for organic matter stabilization then the ξ_{AR} is reduced (Fig. 4) which reduces decomposition rates of fast and slow C pools, reduces their CO_2 emissions, and increases C storage. The forest-mire sites' heterotrophic respiration per unit of area did not show a clear difference between well-drained and water-saturated soils whereas the C mineralization per unit SOC was clearly reduced in soils with mean long term field soil moisture (Fig. 2). Reduction in decomposition rates in the environmental gradient from low to higher field moisture, indicates possible a difference in the soil C stabilization mechanisms under low- and high-water content (Das et al., 2019). Ghezzehei et al. (2019) suggested that empirical moisture sensitivity curves should be calibrated individually for each soil. However, our study shows that the common modifier function, based on the SWC of the topsoil humus layer which has comparable properties across the soil types, could provide insights into a more generalizable moisture sensitivity function. The mechanistic diffusion-based moisture functions (e.g., by Ghezzehei et al., 2019, Yan et al., 2018) could be in follow up studies compared against deterministic moisture functions to evaluate their applicability and interpretation.

The ξ_{AR} function and its reduction with increasing wetness from dry soils was based on a large range of forest/mire soil C stocks (between 11 and 134 kg C m^{-2}) reflecting a spatial long-term moisture gradient between forests and mires (Fig. 2) and its short-term moisture and CO_2 dynamics over years with contrasting climate (Fig. 3). The soil respiration data from three years covered exceptionally contrasting wet and dry summers and likely captured a full range dependency on the soil moisture

induced by short-term weather variation in a spatial/long-term forest-mire gradient in soil moisture, soil C pools, vegetation litter input dynamics (Fig. S2 and S3), and microbial composition. The short-term deviations in respiration indicative of wetting/drying cycles (Barnard et al., 2020; Patel et al., 2021) could be seen by the respiration increases in wet summers or during and after a period of drought (Figure 3). Thus, the $\xi_{AR,p(\theta|SOC-CO2)}$ curve calibrated with highly variable SOC and CO_2 data from a forest-mire ecotone represented a mean robust moisture-decomposition dependency smoothing short-term weather dependent fluctuations with the spatial variation of organic matter decomposition across ecological gradients. This function could meet the land surface modelling criteria for spatial accuracy on small scales but also cost efficiency for running or forecasting the C dynamics at large scales (Luo and Schuur, 2020).

The ξ_{AR} function's SWC_{opt} found in dry conditions and reduction of default decomposition rates (k) with increasing soil wetness contrasted with responses from the short-term laboratory incubation soil respiration studies (weeks, months) showing increase in decomposition from dry conditions until reduction in very wet (Sierra et al., 2017; Moyano et al., 2012, 2013; Kelly et al., 2000; Skopp et al., 1990; Yan et al., 2018). The ξ_{AR} optimized with SOC and CO_2 data showed that the optimum/maximum decomposition rate in the forest-mire ecotone was in dry conditions around 14% of mean long-term near surface SWC (around 20 % WFPS, corresponding to sub-xeric and mesic forest site types) (SWC_{opt} parameters inferred from a parameter in Table 1, Fig. 4b) whereas the moisture optimum of studies based only on soil respiration was around 40% - 60% (Fairbairn et al., 2023; Moyano et al., 2013; Kelly et al., 2000; Skopp et al., 1990; Yan et al., 2018).

The including SOC data or combination of SOC and CO_2 data in model fitting resulted to lower SWC_{opt}, and the model fitting based only on CO_2 showed larger SWC_{opt} and larger tail (descending slope) of the Ricker moisture function. Thus, in comparison to other studies, which dependencies were limited to relatively short-term responses of only soil heterotrophic CO_2 respiration from mainly mineral soils in laboratory conditions, the differences in SWC_{opt} observed in our studies could be expected from difference in data source used in model calibration. Unlike the data from controlled laboratory condition, we used data from field measurements (mineral soil and peat SOC stocks, litter input, soil CO_2 respiration, T_5 and SWC_{10} measured under extreme weather variability during three years. In optimizing model performance with a multi-variable data set, Keenan et al. (2013) found that a combination of data with fast and slow turnover (e.g., soil respiration and soil carbon stocks) leads to the largest improvement in model performance. The Yasso07.ξ_{AR} based only on slow (SOC) was as good as constraining with SOC and CO_2, as both approaches accurately observed soil CO_2 emissions and SOC stocks along the site types of the forest-mire ecotone with no clear bias in residuals (Fig. 6). Thus, in a catena of mineral and peat soils of forest-mire ecotone, and in the combined measured SOC and CO_2 data assimilation in ξ_D (9 and 2369, respectively), the relatively small number of SOC stocks (9 forest/mire types) largely determined the SWC response form reflecting both a spatial moisture gradient and its temporal variation. Whether the deterministic modifier rate was estimated correctly or not also for the drained peatlands should be tested in follow up studies, as our data did not include drained peatlands. The Ricker functional dependency has performed well for the drier region but the performance in soils with high water status still could be improved. This could be deduced

from better statistical performance of CO_2 only fit with CO_2 data (compared to SOC or $SOCCO_2$ fit) which produced larger tail of the Ricker function. Although, the CO_2 only fit also underestimated SOC stocks of forested peatlands.

455 The SWC_{opt} discrepancy of the ξ_{AR} function highlights the difference between (1) the responses from the field-based or long-term soil respiration measurements reflecting moisture responses of older, stabilized and slowly decomposing SOC, and (2) the short-term incubation-based soil respiration studies which predominantly capture decomposition of newly available, labile and rapidly decomposing, SOC pool (González-Domínguez et al., 2022; Huang and Hall, 2017). Over longer periods of incubation high Q_{10} can be observed (Zhou et al., 2019). The enhanced C mineralization can occur during periods of elevated

460 moisture under Fe reduction when microbes can access previously protected labile C (Huang and Hall, 2017).

Although, the moisture representation of the ξ_{AR} environmental function was accurate at the forest-mire ecotone level, at the forest site level the contrasting respiration responses to moisture (i.e., either respiration reduction during soil drying or increased CO_2 emissions with rewetting (Barnard et al., 2020; Patel et al., 2021) for dry soils or the opposite for wet soils), were likely not captured sufficiently. Soil C modelling might be further improved using a moisture response that accounts

465 separately for microbial respiration with increased water availability, and for oxygen limitation in soil reaching water saturation (Sierra et al., 2015). However, as the aim of the environmental modifier used in this study was applying the above concepts in a cost-efficient way using an empirical functions with easily interpretable parameters (Q_{10} and a which informs about SWC optimum) (Davidson et al., 2012), the mathematical representation of the moisture function with increased complexity still needs to be evaluated in further studies testing different functional forms with larger regional data availability. Ghezzehei et

470 al. (2019) suggested that empirical moisture sensitivity curves should be calibrated individually for each soil. The mechanistic diffusion-based moisture functions (e.g., by Moyano et al., 2013, Yan et al., 2018, Ghezzehei et al., 2019) could be in follow up studies tested against deterministic moisture functions (e.g., as in Davidson et al. 2012) to evaluate their applicability and interpretation. However, our study shows that the common modifier function, based on the SWC of the topsoil humus layer which has comparable properties across the soil types, could provide insights into a more generalizable moisture sensitivity

475 function.

4.2 The temperature response

The original air temperature-based modifier in Yasso07 was replaced by the Arrhenius type temperature function driven by soil temperature. This function was found to best represent the enzyme kinetics under unconstrained substrate and oxygen (Sierra et al., 2017). The optimized temperature function with SOC, and combined SOC and CO_2 data produced slightly more

480 biased Rh estimates than modifier based on CO2 data with Q10 around 4.5 (Table 1, Fig. 6). The Q_{10} values around 4.0 were comparable with the well-, moderately-, and poorly- drained forest soils for similar climates (Chen et al., 2020; Davidson et al., 1998; Karhu et al., 2010; Pumpanen et al., 2008). However, the optimization of the Arrhenius type temperature response only with SOC data and SOC and CO_2 with Q_{10} (2.3) (Table 1), showed lower R^2_{adj} values than for the Gaussian type temperature dependency in the Yasso07.ξ_{TW} (Fig. 5). Thus, due to the comparable predictive power when using soil and air

temperature (Jian et al., 2022), the original Gaussian air temperature dependency could be more accurate than Arrhenius response for the optimization with soil temperature (Tuomi et al., 2008).

Discrepancies in modelled respiration during winter (Fig. 6) could be also caused by a scarcity of winter field CO_2 measurements potentially resulting in larger random errors (e.g., due to difficulties of measuring relatively small respiration fluxes during soil freezing/thawing cycles, measurements on soil covered by snow layer, and reduced precision of gas analysers during measurements in lower temperature range).

5   Conclusions

The Yasso07 soil carbon model was developed and parameterized at global scale for mineral soils; however, it has also been applied for land surface modelling coupled with the JSBACH model with a 65% reduction of default decomposition for wetlands. At the forest site level, we evaluated the performance of the Yasso07 model with an original climate modifier based on air temperature and precipitation against the model coupled with a revised environmental modifier based on soil temperature and moisture. We found that the Yasso07 model coupled with revised climate dependencies performed similarly for mineral soils but outperformed the original configuration with the JSBACH modification for undrained peatland soils.

The optimization of moisture dependency conducted in this study accounted for both a spatial moisture gradient and its temporal variation. The moisture optimum at dry soils has not changed depending on whether the function was optimized using both slow (SOC) and fast (CO_2) turnover data or only slow (SOC) data.

The SOC stocks in peatland forests were an order of magnitude larger in comparison to forests on mineral soil. On a landscape level, these peatland SOC stocks had the largest influence on moisture optimum, when they were included along with fluxes in optimization. The function implicitly accounted for relative contribution of C fluxes from short term biogeochemical processes in a long-term SOC accumulation. Thus, for accurate estimates of the boreal forest soil carbon pools with Yasso07 model, the SOC accumulation related to inhibition of decomposition with increasing wetness was more pronounced than the one related to dryness.

This study illustrated the limitation of the default moisture functions used for peatland forest soil C modelling. Also, the unimodal function with a proposed moisture optimum in well-drained mineral soils needs further evaluation with regional boreal forest data. If the dry soil moisture optimum of litter decomposition in boreal forest landscape proves to be robust, then in the future warmer and drier climates the boreal forest could be expected to enhance soil C emissions to the atmosphere due to water level drawdown of presently water-saturated peat soils with large C stocks. However, rewetting of previously drained peatlands could be expected to reduce soil C emissions, turning SOC loss to long-term C sequestration.

6   Data and code availability

The input data (soil CO_2 fluxes, soil temperature and moisture, air temperature and precipitation, tree stand and understory
515   inventory, and soil C stocks) as well as the analysis (R codes) needed to run the Yasso07 model versions and reproduce the
results of this study are available on Zenodo, https://doi.org/10.5281/zenodo.8111475.

7   Author contribution

BT designed the hypothesis, collected data (soil respiration, micrometeorology, tree and understory inventory, and soil C), and
carried out the analysis (input data preparation, the model reformulation on SoilR platform, the model update, calibration, and
520   evaluation). KM contributed to design of the ecological gradient of study sites, and design of measurements of soil respiration
and micrometeorology. AY contributed to soil sampling and soil C data preparation. AL contributed to codes on biomass and
litter estimation. XT contributed to formulation of likelihood for model calibration. BT prepared the manuscript with
contributions from all co-authors.

8   Competing interests

525   We have no conflict of interest to declare.

9   Acknowledgments

The study was partially supported by the SOMPA project (Novel soil management practices - key for sustainable bioeconomy
and climate change mitigation) funded by the Strategic Research Council at the Academy of Finland (no. 312912 and 336570)
and the HoliSoils project (Holistic management practices, modelling and monitoring for European forest soils) funded by
530   European commission (EU Horizon 2020 Grant Agreement No. 101000289).

References

Abramoff, R.Z., Guenet, B., Zhang, H., Georgiou, K., Xu, X., Viscarra Rossel, R.A., Yuan, W., and Ciais, P.: Improved global-
scale predictions of soil carbon stocks with Millennial Version 2. Soil Biology and Biochemistry 164, 108466,
https://doi.org/10.1016/j.soilbio.2021.108466, 2022.

535   Adair, E.C., Parton, W.J., Del Grosso, S.J., Silver, W.L., Harmon, M.E., Hall, S.A., Burke, I.C., and Hart, S.C.: Simple three-
pool model accurately describes patterns of long-term litter decomposition in diverse climates. Global Change Biology 14,
2636–2660, https://doi.org/10.1111/j.1365-2486.2008.01674.x, 2008.

Barnard, R.L., Blazewicz, S.J., and Firestone, M.K.: Rewetting of soil: Revisiting the origin of soil CO2 emissions. Soil
Biology and Biochemistry 147, 107819, https://doi.org/10.1016/j.soilbio.2020.107819, 2020.

540   Berg, B., Booltink, H., Breymeyer, A., Ewertsson, A., Gallardo, A., Holm, B., Johansson, M.-B., Koivuoja, S., Meentemeyer, V., Nyman, P., Olofsson, J., Pettersson, A.-S., Reurslag, A., Staaf, H., Staaf, I., and Uba, L.: Data on needle litter decomposition and soil climate as well as site characteristics for some coniferous forest sites, Part I, Site characteristics. Report 41. Swedish University of Agricultural Sciences, Department of Ecology and Environmental Research, Uppsala, 1991a.

Berg, B., Booltink, H., Breymeyer, A., Ewertsson, A., Gallardo, A., Holm, B., Johansson, M.-B., Koivuoja, S., Meentemeyer, 545   V., Nyman, P., Olofsson, J., Pettersson, A.-S., Reurslag, A., Staaf, H., Staaf, I., and Uba, L.: Data on needle litter decomposition and soil climate as well as site characteristics for some coniferous forest sites, Part II, Decomposition data. Report 42. Swedish University of Agricultural Sciences, Department of Ecology and Environmental Research, Uppsala, 1991b.

Berg, B., Berg, M.P., Bottner, P., Box, E., Breymeyer, A., De Anta, R.C., Couteaux, M., Mälkönen, E., McClaugherty, C., Meentemeyer, V., Munoz, F., Piussi, P., Remacle, J., and De Santo, A.V.: Litter mass loss in pine forests of Europe and Eastern 550   United States: some relationships with climate and litter quality. Biogeochemistry 20, 127–159, https://doi.org/10.1007/BF00000785, 1993.

Bhatti, J., Errington, R., Bauer, I., and Hurdle, P.: Carbon stock trends along forested peatland margins in central Saskatchewan. Canadian Journal of Soil Science 86, 321–333, https://doi.org/10.4141/S05-085, 2006.

Bona, K.A., Shaw, C., Thompson, D.K., Hararuk, O., Webster, K., Zhang, G., Voicu, M., and Kurz, W.A.: The Canadian 555   model for peatlands (CaMP): A peatland carbon model for national greenhouse gas reporting. Ecological Modelling 431, 109164, https://doi.org/10.1016/j.ecolmodel.2020.109164, 2020.

Brooks, S.P., and Gelman, A.: General Methods for Monitoring Convergence of Iterative Simulations. Journal of Computational and Graphical Statistics 7, 434–455, https://doi.org/10.1080/10618600.1998.10474787, 1998.

Cajander A.K.: Forest types and their significance, Acta Forestalia Fennica, 56, 5, https://doi.org/10.14214/aff.7396, 1949.

560   Chadburn, S.E., Burke, E.J., Gallego-Sala, A.V., Smith, N.D., Bret-Harte, M.S., Charman, D.J., Drewer, J., Edgar, C.W., Euskirchen, E.S., Fortuniak, K., Gao, Y., Nakhavali, M., Pawlak, W., Schuur, E.A.G., and Westermann, S.: A new approach to simulate peat accumulation, degradation and stability in a global land surface scheme (JULES vn5.8_accumulate_soil) for northern and temperate peatlands. Geoscientific Model Development 15, 1633–1657, https://doi.org/10.5194/gmd-15-1633-2022, 2022.

565   Chen, S., Wang, J., Zhang, T., Hu, Z.: Climatic, soil, and vegetation controls of the temperature sensitivity (Q10) of soil respiration across terrestrial biomes. Global Ecology and Conservation 22, e00955, https://doi.org/10.1016/j.gecco.2020.e00955, 2020.

Clymo, R.S.: A Model of Peat Bog Growth. In: Heal, O.W., Perkins, D.F. (eds) Production Ecology of British Moors and Montane Grasslands. Ecological Studies, vol 27. Springer, Berlin, Heidelberg. https://doi.org/10.1007/978-3-642-66760-2_9, 570   1978.

Dalsgaard, L., Lange, H., Strand, L.T., Callesen, I., Borgen, S.K., Liski, J., Astrup, R.: Underestimation of boreal forest soil carbon stocks related to soil classification and drainage. Can. J. For. Res. 46, 1413–1425, https://doi.org/10.1139/cjfr-2015-0466, 2016.

575   Das, S., Richards, B.K., Hanley, K.L., Krounbi, L., Walter, M.F., Walter, M.T., Steenhuis, T.S., Lehmann, J.: Lower mineralizability of soil carbon with higher legacy soil moisture. Soil Biology and Biochemistry 130, 94–104, https://doi.org/10.1016/j.soilbio.2018.12.006, 2019.

Davidson, E.A., Samanta, S., Caramori, S.S., and Savage, K.: The Dual Arrhenius and Michaelis–Menten kinetics model for decomposition of soil organic matter at hourly to seasonal time scales. Global Change Biology 18, 371–384, https://doi.org/10.1111/j.1365-2486.2011.02546.x, 2012.

580   Davidson, E., A., Belk, E., Boone, R.D.: Soil water content and temperature as independent or confounded factors controlling soil respiration in a temperate mixed hardwood forest. Global Change Biology 4, 217–227, https://doi.org/10.1046/j.1365-2486.1998.00128.x, 1998.

Dimitrov, D.D., Bhatti, J.S., and Grant, R.F.: The transition zones (ecotone) between boreal forests and peatlands: Ecological controls on ecosystem productivity along a transition zone between upland black spruce forest and a poor forested fen in central

585   Saskatchewan. Ecological Modelling 291, 96–108, https://doi.org/10.1016/j.ecolmodel.2014.07.020, 2014.

Dimitrov, D.D., Lafleur, P., Sonnentag, O., Talbot, J., and Quinton, W.L.: Hydrology of peat estimated from near-surface water contents. Hydrological Sciences Journal 67, 1702-1721, https://doi.org/10.1080/02626667.2022.2099281, 2022.

Falloon, P., Jones, C.D., Ades, M., and Paul, K. Direct soil moisture controls of future global soil carbon changes: An important source of uncertainty. Global Biogeochemical Cycles 25, https://doi.org/10.1029/2010GB003938, 2011.

590   Fairbairn, L., Rezanezhad, F., Gharasoo, M., Parsons, C.T., Macrae, M.L., Slowinski, S., and Van Cappellen, P.: Relationship between soil CO_2 fluxes and soil moisture: Anaerobic sources explain fluxes at high water content. Geoderma 434, 116493, https://doi.org/10.1016/j.geoderma.2023.116493, 2023.

Frolking, S., Roulet, N.T., Moore, T.R., Richard, P.J.H., Lavoie, M., and Muller, S.D.: Modeling Northern Peatland Decomposition and Peat Accumulation. Ecosystems 4, 479–498, https://doi.org/10.1007/s10021-001-0105-1, 2001.

595   Frolking, S., Roulet, N.T., Tuittila, E., Bubier, J.L., Quillet, A., Talbot, J., and Richard, P.J.H.: A new model of Holocene peatland net primary production, decomposition, water balance, and peat accumulation. Earth System Dynamics 1, 1–21, https://doi.org/10.5194/esd-1-1-2010, 2010.

Gao, Y., Markkanen, T., Aurela, M., Mammarella, I., Thum, T., Tsuruta, A., Yang, H., and Aalto, T.: Response of water use efficiency to summer drought in a boreal Scots pine forest in Finland. Biogeosciences 14, 4409–4422,

600   https://doi.org/10.5194/bg-14-4409-2017, 2017.

Ghezzehei, T.A., Sulman, B., Arnold, C.L., Bogie, N.A., Berhe, A.A.: On the role of soil water retention characteristic on aerobic microbial respiration. Biogeosciences 16, 1187–1209. https://doi.org/10.5194/bg-16-1187-2019, 2019.

Gholz, H.L., Wedin, D.A., Smitherman, S.M., Harmon, M.E., and Parton, W.J.: Long-term dynamics of pine and hardwood litter in contrasting environments: toward a global model of decomposition. Global Change Biology 6, 751–765, https://doi.org/10.1046/j.1365-2486.2000.00349.x, 2000.

Goll, D.S., Brovkin, V., Liski, J., Raddatz, T., Thum, T., and Todd-Brown, K.E.O.: Strong dependence of CO_2 emissions from anthropogenic land cover change on initial land cover and soil carbon parametrization. Global Biogeochemical Cycles 29, 1511–1523, https://doi.org/10.1002/2014GB004988, 2015.

González-Domínguez, B., Niklaus, P.A., Studer, M.S., Hagedorn, F., Wacker, L., Haghipour, N., Zimmermann, S., Walthert, L., McIntyre, C., and Abiven, S.: Temperature and moisture are minor drivers of regional-scale soil organic carbon dynamics. Sci Rep 9, 6422, https://doi.org/10.1038/s41598-019-42629-5, 2019.

Han, Q., Zeng, Y., Zhang, L., Wang, C., Prikaziuk, E., Niu, Z., and Su, B.: Global long term daily 1 km surface soil moisture dataset with physics informed machine learning. Sci Data 10, 101, https://doi.org/10.1038/s41597-023-02011-7, 2023.

Hararuk, O., Smith, M.J., and Luo, Y.: Microbial models with data-driven parameters predict stronger soil carbon responses to climate change. Global Change Biology 21, 2439–2453, https://doi.org/10.1111/gcb.12827, 2015.

Hararuk, O., Xia, J., and Luo, Y.: Evaluation and improvement of a global land model against soil carbon data using a Bayesian Markov chain Monte Carlo method. Journal of Geophysical Research: Biogeosciences 119, 403–417, https://doi.org/10.1002/2013JG002535, 2014.

Hartig, F., Dyke, J., Hickler, T., Higgins, S.I., O'Hara, R.B., Scheiter, S., and Huth, A.: Connecting dynamic vegetation models to data – an inverse perspective. Journal of Biogeography 39, 2240–2252. https://doi.org/10.1111/j.1365-2699.2012.02745.x, 2012.

Hartig, F., Minunno, F., Paul, S., Cameron, D., Ott, T., and Pichler, M.: BayesianTools: General-Purpose MCMC and SMC Samplers and Tools for Bayesian Statistics, https://CRAN.R-project.org/package=BayesianTools, 2019.

Hartshorn, A.S., Southard, R.J., and Bledsoe, C.S.: Structure and Function of Peatland-Forest Ecotones in Southeastern Alaska. Soil Science Society of America Journal 67, 1572–1581, https://doi.org/10.2136/sssaj2003.1572, 2003.

Hashimoto, S., Morishita, T., Sakata, T., Ishizuka, S., Kaneko, S., and Takahashi, M.: Simple models for soil CO_2, CH_4, and N_2O fluxes calibrated using a Bayesian approach and multi-site data. Ecological Modelling 222, 1283–1292, https://doi.org/10.1016/j.ecolmodel.2011.01.013, 2011.

Hashimoto, S., Nanko, K., Ťupek, B., Lehtonen, A.: Data-mining analysis of the global distribution of soil carbon in observational databases and Earth system models. Geoscientific Model Development 10, 1321–1337, https://doi.org/10.5194/gmd-10-1321-2017, 2017.

Huang, W., and Hall, S.J.: Elevated moisture stimulates carbon loss from mineral soils by releasing protected organic matter. Nat Commun 8, 1774, https://doi.org/10.1038/s41467-017-01998-z, 2017.

Humphrey, V., Berg, A., Ciais, P., Gentine, P., Jung, M., Reichstein, M., Seneviratne, S.I., and Frankenberg, C.: Soil moisture–atmosphere feedback dominates land carbon uptake variability. Nature 592, 65–69, https://doi.org/10.1038/s41586-021-03325-5, 2021.

Jian, J., Steele, M.K., Zhang, L., Bailey, V.L., Zheng, J., Patel, K.F., and Bond-Lamberty, B.P.: On the use of air temperature and precipitation as surrogate predictors in soil respiration modelling. European Journal of Soil Science 73, e13149, https://doi.org/10.1111/ejss.13149, 2022.

Karhu, K., Fritze, H., Hämäläinen, K., Vanhala, P., Jungner, H., Oinonen, M., Sonninen, E., Tuomi, M., Spetz, P., Kitunen, V., Liski, J.: Temperature sensitivity of soil carbon fractions in boreal forest soil. Ecology 91, 370–376, https://www.jstor.org/stable/25661063, 2010.

Keenan, T.F., Davidson, E.A., Munger, J.W., and Richardson, A.D.: Rate my data: quantifying the value of ecological data for the development of models of the terrestrial carbon cycle. Ecological Applications 23, 273–286, https://doi.org/10.1890/12-0747.1, 2013.

Kelly, R.H., Parton, W.J., Hartman, M.D., Stretch, L.K., Ojima, D.S., and Schimel, D.S.: Intra-annual and interannual variability of ecosystem processes in shortgrass steppe. Journal of Geophysical Research: Atmospheres 105, 20093–20100, https://doi.org/10.1029/2000JD900259, 2000.

Kleinen, T., Brovkin, V., and Schuldt, R.J.: A dynamic model of wetland extent and peat accumulation: results for the Holocene. Biogeosciences 9, 235–248, https://doi.org/10.5194/bg-9-235-2012, 2012.

Kleinen, T., Gromov, S., Steil, B., and Brovkin, V.: Atmospheric methane underestimated in future climate projections. Environ. Res. Lett. 16, 094006, https://doi.org/10.1088/1748-9326/ac1814, 2021.

Laine, J., Komulainen, V.M., Laiho, R., Minkkinen, K., Rasinmaki, A., Sallantaus, T., Sarkkola, S., Silvan, N., Tolonen, K., Tuittila, E.S., Vasander, H., and Paivanen, J.: Lakkasuo: a guide to mire ecosystem, Helsingin yliopiston metsäekologian laitoksen julkaisuja. Helsingin yliopisto, metsäekologian laitos, Helsinki, 2004.

Launiainen, S., Guan, M., Salmivaara, A., and Kieloaho, A.-J.: Modeling boreal forest evapotranspiration and water balance at stand and catchment scales: a spatial approach. Hydrology and Earth System Sciences 23, 3457–3480, https://doi.org/10.5194/hess-23-3457-2019, 2019.

Lehtonen, A., Linkosalo, T., Peltoniemi, M., Sievänen, R., Mäkipää, R., Tamminen, P., Salemaa, M., Nieminen, T., Ťupek, B., Heikkinen, J., and Komarov, A.: Forest soil carbon stock estimates in a nationwide inventory: evaluating performance of the ROMULv and Yasso07 models in Finland. Geoscientific Model Development 9, 4169–4183. https://doi.org/10.5194/gmd-9-4169-2016, 2016.

Leifeld, J., Menichetti, L.: The underappreciated potential of peatlands in global climate change mitigation strategies. Nat Commun 9, 1071, https://doi.org/10.1038/s41467-018-03406-6, 2018.

Leppä, K., Hökkä, H., Laiho, R., Launiainen, S., Lehtonen, A., Mäkipää, R., Peltoniemi, M., Saarinen, M., Sarkkola, S., and Nieminen, M.: Selection Cuttings as a Tool to Control Water Table Level in Boreal Drained Peatland Forests. Frontiers in Earth Science 8. https://doi.org/10.3389/feart.2020.576510Luo, Y., Ogle, K., Tucker, C., Fei, S., Gao, C., LaDeau, S., Clark, J.S., Schimel, D.S., 2011. Ecological forecasting and data assimilation in a data-rich era. Ecological Applications 21, 1429–1442, https://doi.org/10.1890/09-1275.1, 2020.

Luo, Y., and Schuur, E.A.G.: Model parameterization to represent processes at unresolved scales and changing properties of evolving systems. Global Change Biology 26, 1109–1117, https://doi.org/10.1111/gcb.14939, 2020.

Manzoni, S., Schimel, J.P., and Porporato, A.: Responses of soil microbial communities to water stress: results from a meta-analysis. Ecology 93, 930–938, https://doi.org/10.1890/11-0026.1, 2012.

Metherell, A.K., Harding, L.A., Cole, C.V., and Parton, W.J.: CENTURY Soil Organic Matter Model Environment Technical Documentation, Agroecosystem Version 4.0, Great Plains System Research Unit, Technical Report No. 4. USDA-ARS, Ft. Collins. https://www2.nrel.colostate.edu/projects/century/MANUAL/html_manual/man96.html, 1993.

Moyano, F.E., Vasilyeva, N., Bouckaert, L., Cook, F., Craine, J., Curiel Yuste, J., Don, A., Epron, D., Formanek, P., Franzluebbers, A., Ilstedt, U., Kätterer, T., Orchard, V., Reichstein, M., Rey, A., Ruamps, L., Subke, J.-A., Thomsen, I.K., and Chenu, C.: The moisture response of soil heterotrophic respiration: interaction with soil properties. Biogeosciences 9, 1173–1182, https://doi.org/10.5194/bg-9-1173-2012, 2012.

Parton, W.J.: The CENTURY model, in: Powlson, D.S., Smith, P., Smith, J.U. (Eds.), Evaluation of Soil Organic Matter Models, NATO ASI Series. Springer, Berlin, Heidelberg, 283–291, https://doi.org/10.1007/978-3-642-61094-3_23, 1996.

Patel, K.F., Myers-Pigg, A., Bond-Lamberty, B., Fansler, S.J., Norris, C.G., McKever, S.A., Zheng, J., Rod, K.A., and Bailey, V.L.: Soil carbon dynamics during drying vs. rewetting: Importance of antecedent moisture conditions. Soil Biology and Biochemistry 156, 108165, https://doi.org/10.1016/j.soilbio.2021.108165, 2021.

Pumpanen, J., Ilvesniemi, H., Kulmala, L., Siivola, E., Laakso, H., Kolari, P., Helenelund, C., Laakso, M., Uusimaa, M., Hari, P.: Respiration in Boreal Forest Soil as Determined from Carbon Dioxide Concentration Profile. Soil Science Society of America Journal 72, 1187–1196, https://doi.org/10.2136/sssaj2007.0199, 2008.

690 Qiu, C., Zhu, D., Ciais, P., Guenet, B., Krinner, G., Peng, S., Aurela, M., Bernhofer, C., Brümmer, C., Bret-Harte, S., Chu, H., Chen, J., Desai, A.R., Dušek, J., Euskirchen, E.S., Fortuniak, K., Flanagan, L.B., Friborg, T., Grygoruk, M., Gogo, S., Grünwald, T., Hansen, B.U., Holl, D., Humphreys, E., Hurkuck, M., Kiely, G., Klatt, J., Kutzbach, L., Largeron, C., Laggoun-Défarge, F., Lund, M., Lafleur, P.M., Li, X., Mammarella, I., Merbold, L., Nilsson, M.B., Olejnik, J., Ottosson-Löfvenius, M., Oechel, W., Parmentier, F.-J.W., Peichl, M., Pirk, N., Peltola, O., Pawlak, W., Rasse, D., Rinne, J., Shaver, G., Schmid, H.P., Sottocornola, M., Steinbrecher, R., Sachs, T., Urbaniak, M., Zona, D., and Ziemblinska, K.: ORCHIDEE-PEAT (revision
695 4596), a model for northern peatland CO2, water, and energy fluxes on daily to annual scales. Geoscientific Model Development 11, 497–519, https://doi.org/10.5194/gmd-11-497-2018, 2018.

R Core Team: R: A language and environment for statistical computing. R Foundation for Statistical Computing, Vienna, Austria. https://www.R-project.org/, 2023.

Raich, J.W., Parton, W.J., Russell, A.E., Sanford, R.L., and Vitousek, P.M.: Analysis of factors regulating
700 ecosystemdevelopment on Mauna Loa using the Century model. Biogeochemistry 51, 161–191, https://doi.org/10.1023/A:1006495408992, 2000.

Scharlemann, J.P., Tanner, E.V., Hiederer, R., and Kapos, V.: Global soil carbon: understanding and managing the largest terrestrial carbon pool. Carbon Management 5, 81–91, https://doi.org/10.4155/cmt.13.77, 2014.

Schuur, E. a. G., McGuire, A.D., Schädel, C., Grosse, G., Harden, J.W., Hayes, D.J., Hugelius, G., Koven, C.D., Kuhry, P.,
705 Lawrence, D.M., Natali, S.M., Olefeldt, D., Romanovsky, V.E., Schaefer, K., Turetsky, M.R., Treat, C.C., and Vonk, J.E.: Climate change and the permafrost carbon feedback. Nature 520, 171–179, https://doi.org/10.1038/nature14338, 2015.

Sierra, C.A., Malghani, S., and Loescher, H.W.: Interactions among temperature, moisture, and oxygen concentrations in controlling decomposition rates in a boreal forest soil. Biogeosciences 14, 703–710, https://doi.org/10.5194/bg-14-703-2017, 2017.

710 Sierra, C.A., Müller, M., and Trumbore, S.E.: Models of soil organic matter decomposition: the SoilR package, version 1.0. Geoscientific Model Development 5, 1045–1060, https://doi.org/10.5194/gmd-5-1045-2012, 2012.

Sierra, C.A., Trumbore, S.E., Davidson, E.A., Vicca, S., and Janssens, I.: Sensitivity of decomposition rates of soil organic matter with respect to simultaneous changes in temperature and moisture. Journal of Advances in Modeling Earth Systems 7, 335–356, https://doi.org/10.1002/2014MS000358, 2015.

715 Skopp, J., Jawson, M.D., and Doran, J.W.: Steady-State Aerobic Microbial Activity as a Function of Soil Water Content. Soil Science Society of America Journal 54, 1619–1625, https://doi.org/10.2136/sssaj1990.03615995005400060018x, 1990.

Speich, M., Dormann, C.F., and Hartig, F.: Sequential Monte-Carlo algorithms for Bayesian model calibration – A review and method comparison. Ecological Modelling 455, 109608, https://doi.org/10.1016/j.ecolmodel.2021.109608, 2021.

Statistics Finland: Greenhouse gas emissions in Finland 1990 to 2021. National Inventory Report under the UNFCCC and the Kyoto Protocol, Statistics Finland, Retrieved May 15, 2023, https://www.stat.fi/static/media/uploads/tup/khkinv/fi_nir_eu_2021_2023-03-15.pdf, 2023.

St-Hilaire, F., Wu, J., Roulet, N.T., Frolking, S., Lafleur, P.M., Humphreys, E.R., and Arora, V.: McGill wetland model: evaluation of a peatland carbon simulator developed for global assessments. Biogeosciences 7, 3517–3530, https://doi.org/10.5194/bg-7-3517-2010, 2010.

Straková, P., Anttila, J., Spetz, P., Kitunen, V., Tapanila, T., and Laiho, R.: Litter quality and its response to water level drawdown in boreal peatlands at plant species and community level. Plant Soil 335, 501–520, https://doi.org/10.1007/s11104-010-0447-6, 2010.

ter Braak, C.J.F., and Vrugt, J.A.: Differential Evolution Markov Chain with snooker updater and fewer chains. Stat Comput 18, 435–446, https://doi.org/10.1007/s11222-008-9104-9, 2008.

Thum, T., Nabel, J.E.M.S., Tsuruta, A., Aalto, T., Dlugokencky, E.J., Liski, J., Luijkx, I.T., Markkanen, T., Pongratz, J., Yoshida, Y., and Zaehle, S.: Evaluating two soil carbon models within the global land surface model JSBACH using surface and spaceborne observations of atmospheric CO_2. Biogeosciences 17, 5721–5743, https://doi.org/10.5194/bg-17-5721-2020, 2020.

Todd-Brown, K.E.O., Randerson, J.T., Post, W.M., Hoffman, F.M., Tarnocai, C., Schuur, E. a. G., and Allison, S.D.: Causes of variation in soil carbon simulations from CMIP5 Earth system models and comparison with observations. Biogeosciences 10, 1717–1736, https://doi.org/10.5194/bg-10-1717-2013, 2013.

Trofymow, J.A.: The Canadian Intersite Decomposition ExperimenT (CIDET). Project and site establishment report. Information report BCX-378. Pacific Forestry Centre, Victoria, Canada, 1998.

Tuomi, M., Laiho, R., Repo, A., and Liski, J.: Wood decomposition model for boreal forests. Ecological Modelling 222, 709–718, https://doi.org/10.1016/j.ecolmodel.2010.10.025, 2011.

Tuomi, M., Thum, T., Järvinen, H., Fronzek, S., Berg, B., Harmon, M., Trofymow, J.A., Sevanto, S., and Liski, J.: Leaf litter decomposition—Estimates of global variability based on Yasso07 model. Ecological Modelling 220, 3362–3371. https://doi.org/10.1016/j.ecolmodel.2009.05.016, 2009.

Tuomi, M., Vanhala, P., Karhu, K., Fritze, H., and Liski, J.: Heterotrophic soil respiration—Comparison of different models describing its temperature dependence. Ecological Modelling 211, 182–190, https://doi.org/10.1016/j.ecolmodel.2007.09.003, 2008.

Ťupek, B., Launiainen, S., Peltoniemi, M., Sievänen, R., Perttunen, J., Kulmala, L., Penttilä, T., Lindroos, A.-J., Hashimoto, S., and Lehtonen, A.: Evaluating CENTURY and Yasso soil carbon models for CO_2 emissions and organic carbon stocks of

boreal forest soil with Bayesian multi-model inference. European Journal of Soil Science 70, 847–858. https://doi.org/10.1111/ejss.12805, 2019.

Ťupek, B., Minkkinen, K., Kolari, P., Starr, M., Chan, T., Alm, J., Vesala, T., Laine, J., Nikinmaa, E.: Forest floor versus ecosystem CO2 exchange along boreal ecotone between upland forest and lowland mire. Tellus B: Chemical and Physical Meteorology 60, 153–166. https://doi.org/10.1111/j.1600-0889.2007.00328.x, 2008.

Tupek, B., Minkkinen, K., Pumpanen, J., Vesala, T., and Nikinmaa, E.: CH4 and N2O dynamics in the boreal forest–mire ecotone. Biogeosciences 12, 281–297. https://doi.org/10.5194/bg-12-281-2015, 2015.

Vávřová, P., Penttilä, T., and Laiho, R.: Decomposition of Scots pine fine woody debris in boreal conditions: Implications for estimating carbon pools and fluxes. Forest Ecology and Management 257, 401–412, https://doi.org/10.1016/j.foreco.2008.09.017, 2009.

Wania, R., Ross, I., and Prentice, I.C.: Implementation and evaluation of a new methane model within a dynamic global vegetation model: LPJ-WHyMe v1.3.1. Geoscientific Model Development 3, 565–584, https://doi.org/10.5194/gmd-3-565-2010, 2010.

Weishampel, P., Kolka, R., and King, J.Y.: Carbon pools and productivity in a 1-km2 heterogeneous forest and peatland mosaic in Minnesota, USA. Forest Ecology and Management 257, 747–754, https://doi.org/10.1016/j.foreco.2008.10.008, 2009.

Xia, J.Y., Luo, Y.Q., Wang, Y.-P., Weng, E.S., Hararuk, O.: A semi-analytical solution to accelerate spin-up of a coupled carbon and nitrogen land model to steady state. Geoscientific Model Development 5, 1259–1271. https://doi.org/10.5194/gmd-5-1259-2012, 2012.

Xu, T., White, L., Hui, D., Luo, Y.: Probabilistic inversion of a terrestrial ecosystem model: Analysis of uncertainty in parameter estimation and model prediction. Global Biogeochemical Cycles 20, https://doi.org/10.1029/2005GB002468, 2006.

Yan, Z., Bond-Lamberty, B., Todd-Brown, K.E., Bailey, V.L., Siliang, L, Congqiang, L, and Chongxuan, L.: A moisture function of soil heterotrophic respiration that incorporates microscale processes. Nat Commun 9, 2562, https://doi.org/10.1038/s41467-018-04971-6, 2018.

Zhou, W., Hui, D., and Shen, W.: Effects of Soil Moisture on the Temperature Sensitivity of Soil Heterotrophic Respiration: A Laboratory Incubation Study. PLOS ONE 9, e92531. https://doi.org/10.1371/journal.pone.0092531, 2014.

775
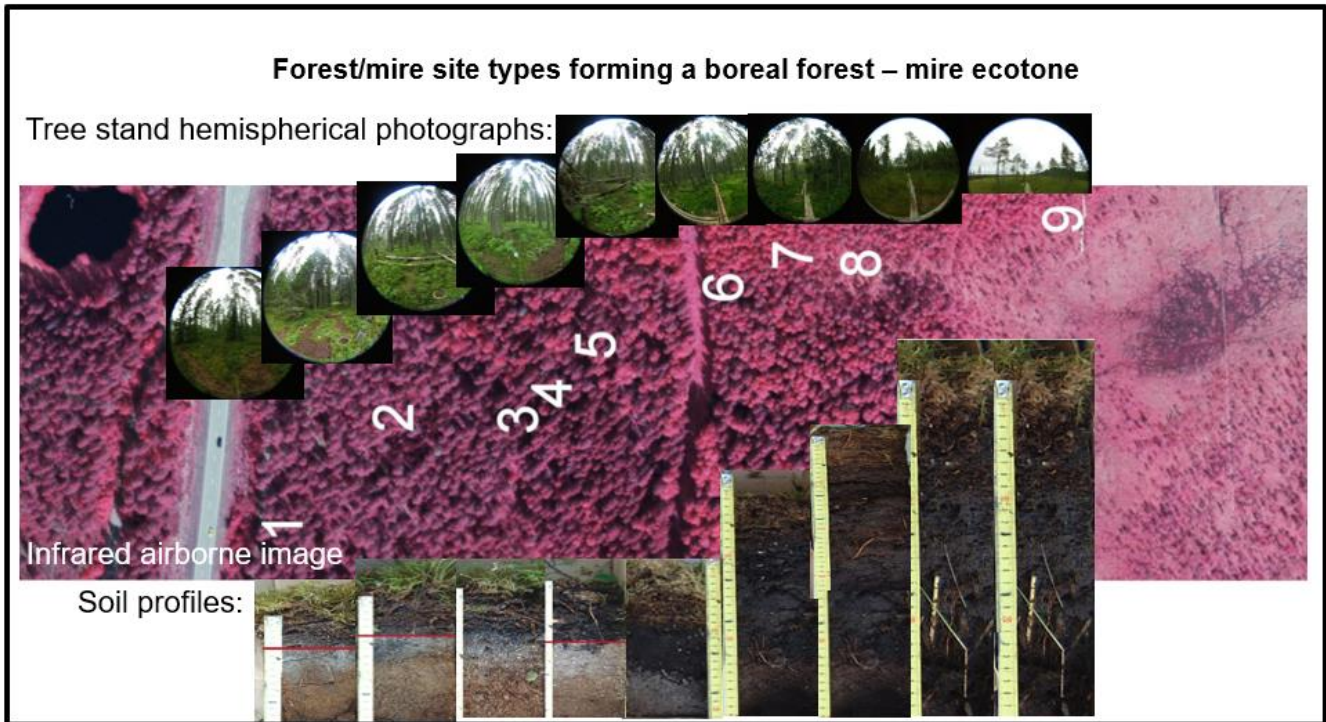
Figure 1. Infrared areal image showing the location of nine studied forest/mire types forming a transect of approximately 450 m on the northern hillslope in Finland (61° 47', 24° 19'). The series of hemispherical images of forest stands on the top of the aerial image show the increasing gradient in the canopy openness from upland forests (left) to mires (right). The series of soil profiles show the increasing gradient of the organic layer depth. The images in the series arranged from left to right mimic the site type location on the slope from the hill to depression. Sites range from upland (1) xeric, (2) sub-xeric, (3) mesic and (4) herb-rich forest types (CT - Calluna, VT - Vitis Idaea, MT - Myrtilus, OMT - Oxalis-Myrtillus), through paludified forest - mire transitions (5 - 7) (OMT+ - Oxalis-Myrtillus Paludified, KgK – Myrtillus Spruce Forest Paludified, KR – Spruce Pine Swamp), to sparsely forested mires/peatlands in depression (8 - 9) (VSR1 and VSR2 - Tall Sedge Pine Fen).

780
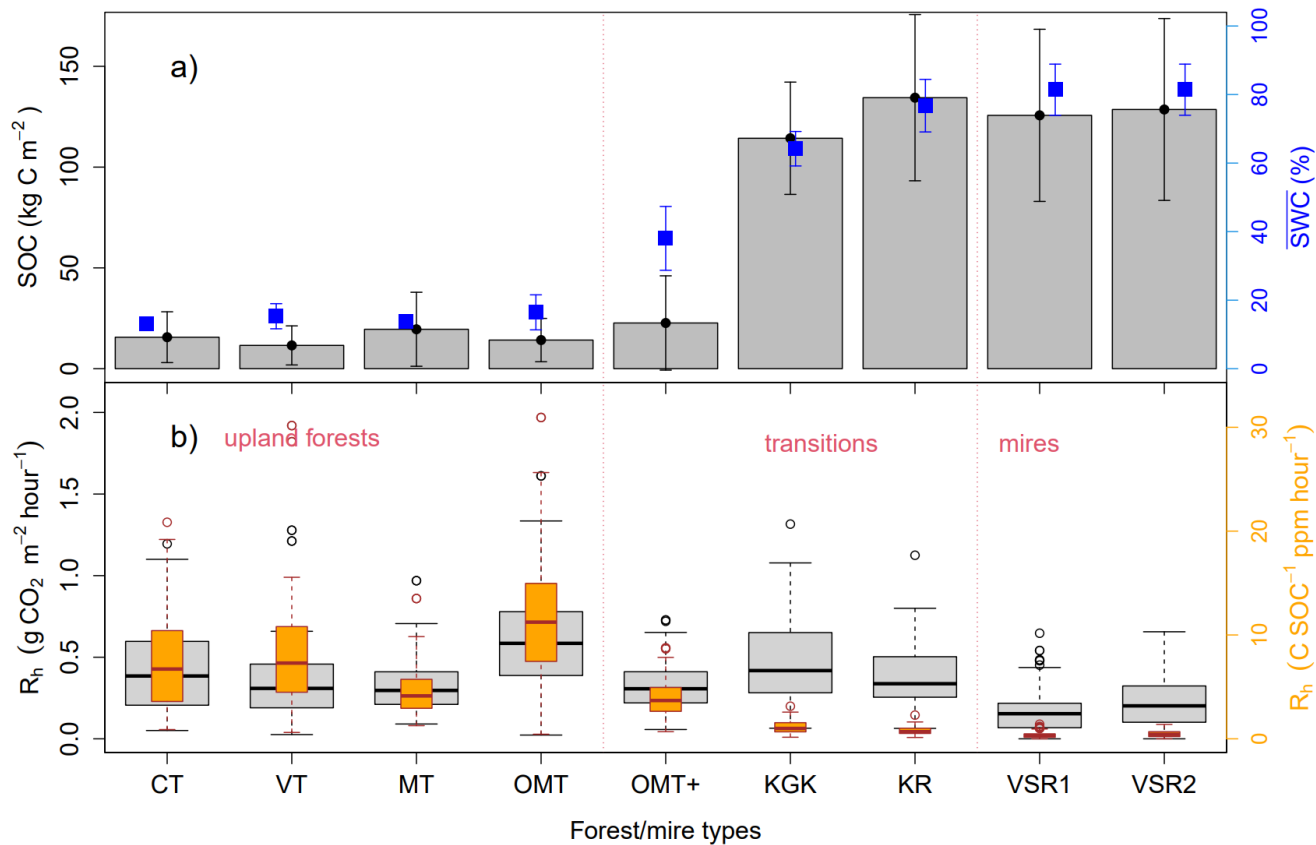
Figure 2. Forest/mire site type specific observations of soil organic carbon (SOC) stocks (kg C m^{-2}, summed up to 1 m) and the mean volumetric soil water content (SWC) at 10 cm depth (%) (with error bars showing one standard deviation) (a) in comparison to their distributions of heterotrophic soil CO_2 emissions/respiration measurements (Rh, gCO_2 m^{-2} h^{-1}) and R$_h$ expressed as the emitted C fraction per site specific SOC stock (C SOC^{-1} ppm h^{-1}) (b). The CT, VT, MT, and OMT types represent upland forests, OMT+, KgK, and KR forest-mire transitions, and VSR1 and VSR2 mires. The boxplot horizontal lines show 25th and 75th interval with median in between, and 5th and 95th confidence interval (whiskers).
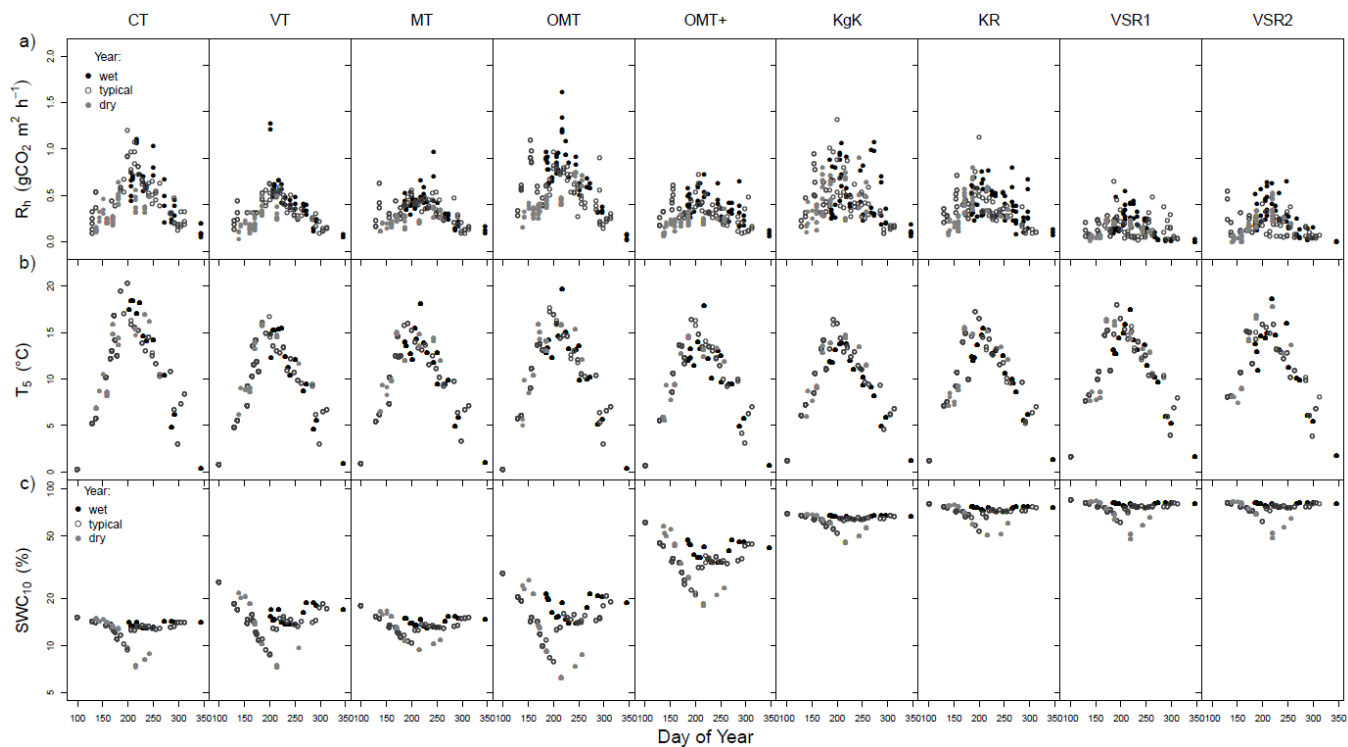
Figure 3. The three years' time series (2004 - wet, 2005 - typical, and 2006 - dry) of instantaneous measurements of a) soil heterotrophic respiration (R_h, gCO$_2$ m^{-2} h^{-1}, positive sign), b) soil temperature at 5 cm depth (°C), and c) soil moisture at 10 cm depth (%)) of 9 forest/mire sites (4 upland forests (CT,MT, and OMT), 3 forest-mire transitions (OMT+, KgK, and KR) and 2 mires (VSR1 and VSR2). The sites are arranged from left to right according to their position on the slope (see Fig. 1).

795
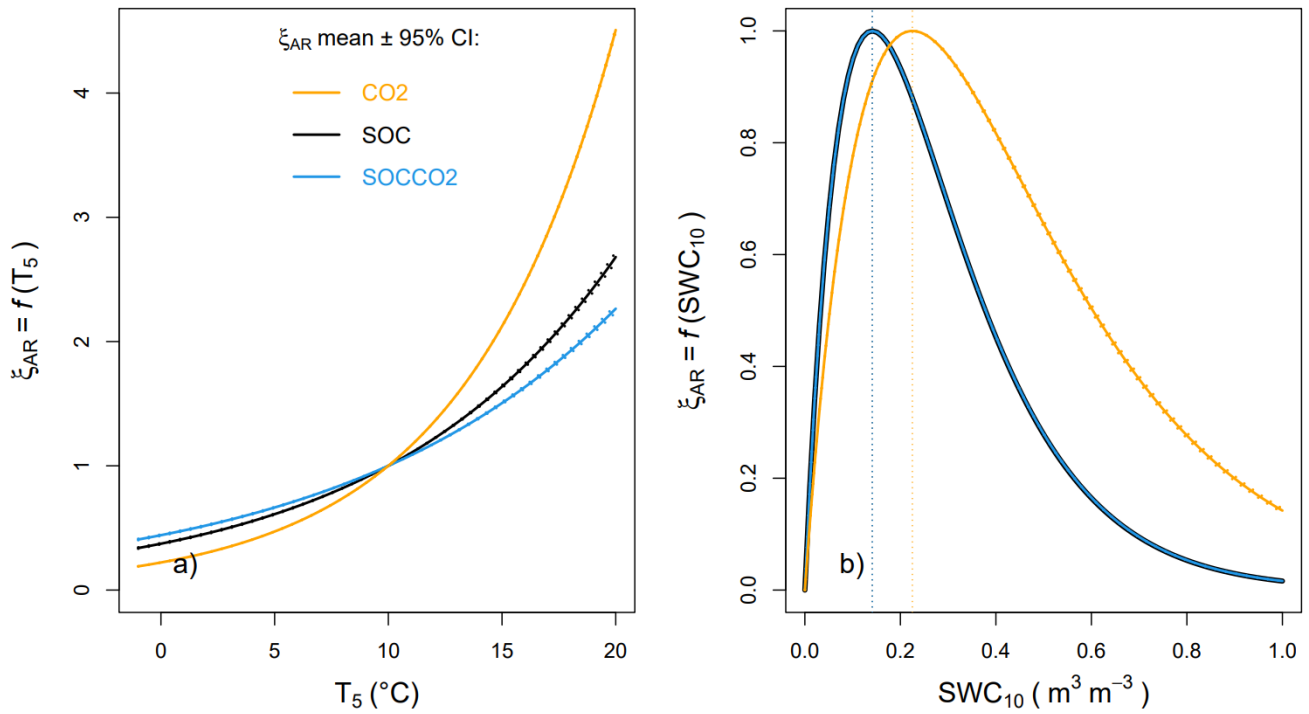
Figure 4. The optimized environmental modifier of default decomposition rates ξ_{AR} (Eq. (3)) (coupled with Yasso07 model) drawn with mean posterior values of parameters and their confident intervals (dashed lines) (Table 1) for separate responses to (a) soil temperature at 5 cm, ξ_{AR} = f(T_5) when f(SWC_{10}) = 1, (b) to soil water content at 10 cm, ξ_{AR} = f(SWC_{10}) when f(T_5) = 1. The functions were fitted based on only CO_2, SOC and CO_2, or only SOC data.
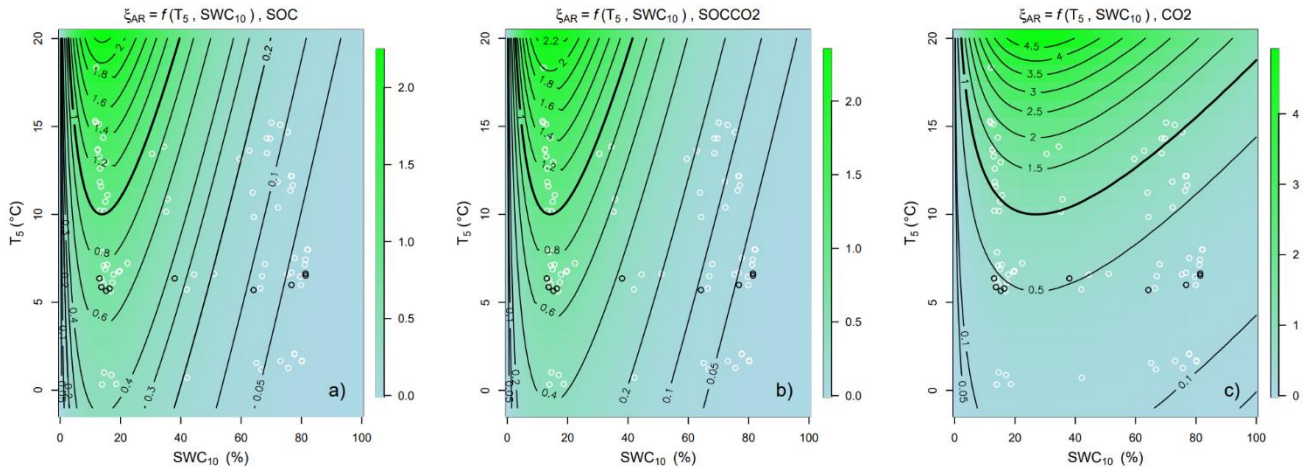
Figure 5. The optimized environmental modifier of default decomposition rates ξ_D (Eq. (3)) (coupled with Yasso07 model) drawn with mean posterior values of parameters (Table 1) for combined responses to soil temperature at 5 cm, $\xi_{AR} = f(T_5)$ and to soil water content at 10 cm, $\xi_D = f(SWC_{10})$ based on only SOC (a), SOC and CO_2 (b), or only CO_2 (c) data.
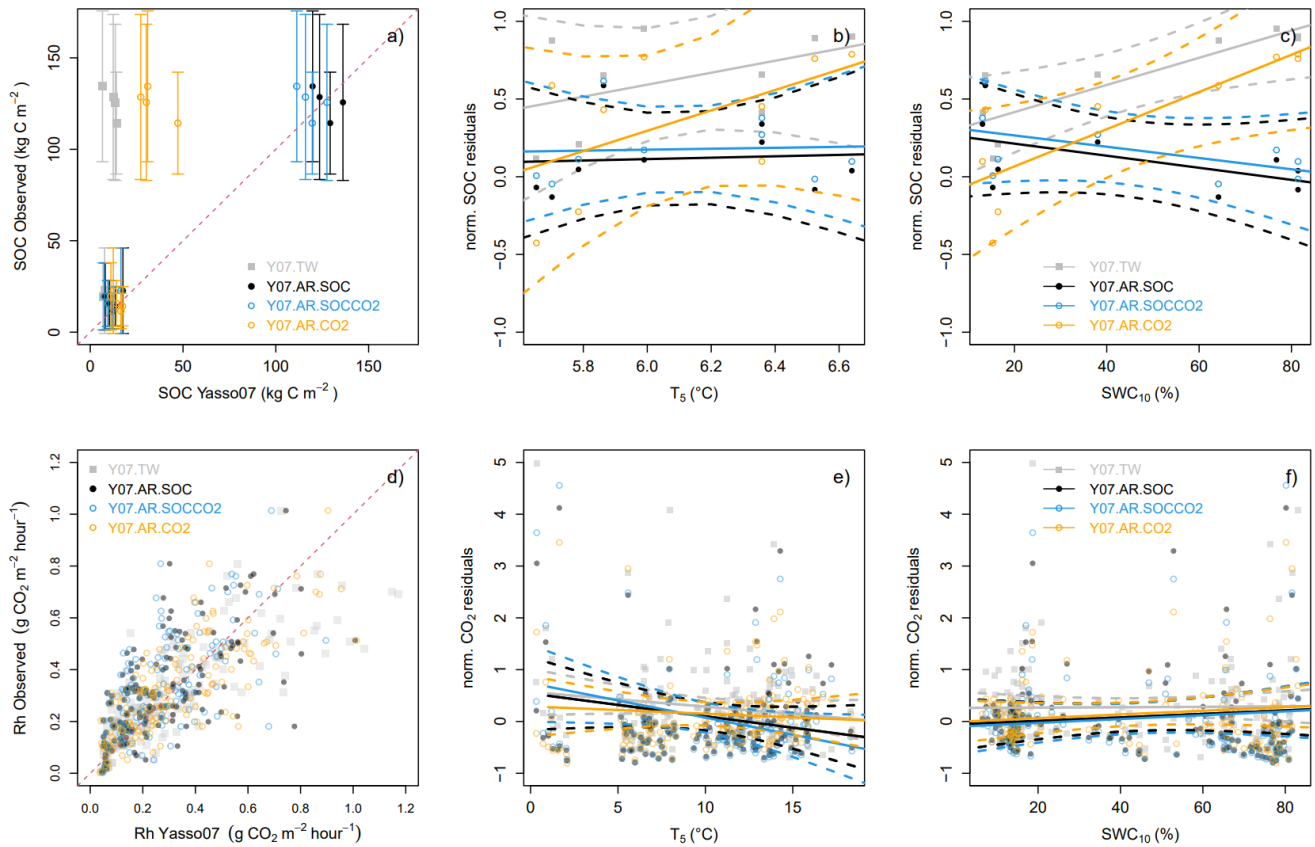
Figure 6. Scatterplots between observed SOC (kg C m^{-2}) and Rh (g CO$_2$ m^{-2} hour^{-1}) from the forest-mire ecotone against
modelled values with the two versions of Yasso07 model (i) Y07.ξ_{TW} – Yasso07 coupled with the default environmental
modifier (ξ_T, Eq. (3)) based on air T and precipitation with global parameter set (Tuomi et al., 2011) (applied for CT…KR
mineral and organo-mineral soil forest sites) and with the reduction of decomposition rates by 65% for wetlands (Goll et al.,
2015, Kleinen et al., 2021) (applied for VSR1, VSR2 mires sites), and (ii) Y07.ξ_{AR} - Yasso07 coupled with environmental
modifier (ξ_{AR}, Eq.3) based on based on SOC, SOC-CO2, or CO2 data (a, d) compared with 1:1 line (dashed red line). The
model residuals normalized with the observations (norm. SOC and CO$_2$ residuals = residuals/observations) are plotted against
the T$_5$ and SWC$_{10}$ with the trendlines of the linear fits and with their confident intervals (dashed lines) (b, c, e, and f).

Table 1. The posterior distribution of parameters of Yasso07 soil carbon model (parameters same as in Table S1) coupled with environmental function ξ_D (Eq. (3), parameters d, Q_{10}, SWC_{opt}) optimized with observations of SOC stocks (p (θ | SOC)) or SOC stocks and CO_2 emissions (p (θ | SOC-CO2)) from forest/mire ecotone sites using Bayesian data assimilation (Hartig et al., 2012). The PSRF stands for Gelman–Rubin potential scale reduction factor and MAP for a maximum a posteriori probability. $1/ae^{-1}$. The SWC_{10} optimum (the SWC_{10} when the SOC decomposition in the foreal forest -mire ecotone was at optimum) was inferred as $1/ae^{-1}$ and ranged between 14 and 27 % (for $a_{MAP\ SOC}$ and $a_{MAP\ CO2}$, respectively).

Posterior p(θ | data)	ξ_{AR} parameters	PSRF	MAP	2.50 %	50 %	97.50 %
SOC	Q_{10}	1.001	2.239	1.157	2.503	4.72
SOC	a	1.001	19.576	18.172	19.271	20.538
SOC	ae1	1.002	0.099	0.032	0.077	0.099
SOC	be1	1.001	0	0	0	0.002
SOC, CO_2	Q_{10}	1.016	2.342	1.611	2.213	3.103
SOC, CO_2	a	1.015	19.15	18.725	19.261	19.93
SOC, CO_2	ae1	1.017	0.015	0.011	0.029	0.121
SOC, CO_2	be1	1.024	0.01	0.01	0.01	0.012
SOC, CO_2	ae2	1.018	0.5	0.453	0.496	0.5
SOC, CO_2	be2	1.026	0.995	0.337	0.982	0.999
CO_2	Q_{10}	1.004	4.897	3.525	4.57	4.982
CO_2	a	1.001	10.066	10.07	11.741	16.21
CO_2	ae	1.008	0.5	0.48	0.496	0.5
CO_2	be	1.01	0.999	0.923	0.986	0.999

Table 2. The SOC and CO_2 performance statistics of Yasso07 (Y07) model versions against the measured data in boreal forest-mire ecotone where N is the number of observations, MAE is the mean absolute error, MBE is the mean bias error, RMSE is the root mean square error, R^2_{adj} is the adjusted coefficient of determination, and AIC is the Akaike Information Criterion. The units of MAE, MBE, and RMSE are in kg C m^{-2} and kg CO_2 m^{-2} month^{-1} for SOC and CO_2, respectively.

Data	Yasso07 model	MBE	MAE	RMSE	R^2_{adj}	AIC
SOC	Y07.ξ_{TW}	-54.97	54.97	76.67	0.05	87.06
SOC	Y07. $\xi_{AR.SOC}$	-1.76	7.59	9.18	0.97	65.95
SOC	Y07. $\xi_{AR.SOCCO2}$	-6.03	7.63	10.25	0.97	66.95
SOC	Y07. $\xi_{AR.CO2}$	-42.17	43.98	62.2	0.63	83.17
CO_2	Y07.ξ_{TW}	0.01	0.11	0.16	0.6	-233.65
CO_2	Y07. $\xi_{AR.SOC}$	-0.04	0.12	0.16	0.44	-237.37
CO_2	Y07. $\xi_{AR.SOCCO2}$	-0.06	0.12	0.16	0.44	-238.31
CO_2	Y07. $\xi_{AR.CO2}$	0	0.1	0.13	0.63	-266.9